PINGUID, THE DROSOPHILA HOMOLOG OF HUNTINGTIN INTERACTING PROTEIN 14, ENCODES AN ESSENTIAL PROTEIN INVOLVED IN TGF BETA SIGNALLING

by

Bryan Andrews
B.Sc. Simon Fraser University, 1998

THESIS SUBMITTED IN PARTIAL FULFILLMENT OF
THE REQUIREMENTS FOR THE DEGREE OF
MASTER OF SCIENCE

In the Department of
Molecular Biology and Biochemistry

SIMON FRASER UNIVERSITY
Spring 2006

Your file Votre référence
ISBN: 978-0-494-24027-4
Our file Notre référence
ISBN: 978-0-494-24027-4

APPROVAL

Name: Bryan Andrews

Degree: Master of Science

Title of Thesis: *pinguid*, the Drosophila homolog of Huntingtin Interacting Protein 14, encodes an essential protein involved in TGF beta Signalling

Examining Committee:

Chair: Dr. N. Haunerland, Professor
Department of Biological Sciences, SFU

Dr. E. Verheyen, Associate Professor, Senior Supervisor
Department of Molecular Biology and Biochemistry, SFU

Dr. N. Harden, Associate Professor, Committee member
Department of Molecular Biology and Biochemistry, SFU

Dr. C. Beh, Assistant Professor, Committee member
Department of Molecular Biology and Biochemistry, SFU

Dr. L. Quarmby, Associate Professor, Public Examiner
Department of Molecular Biology and Biochemistry, SFU

Date Approved: December 6, 2005

ABSTRACT

To elucidate the cellular function of Huntingtin interacting protein 14 (Hip14), a genetic approach using Drosophila was initiated. The gene encoding Pinguid was identified as the closest Drosophila homolog to human Hip14 with 44% identity and 59% similarity. A P-element insertion in the 5' UTR of *pinguid* was used for carrying out a transposase mediated P-element excision screen. Subsequent genetic and molecular experiments confirmed that *pinguid* encodes an essential gene. Five *pinguid* alleles were identified: three excision alleles and two EMS-induced alleles. No visible defects were observed in the mutants since the morphology and patterning of the embryos appeared normal, CNS development appeared wild type, and pharate adults had no visible external defects. However, the ectopic expression of *pinguid* identified genetic interactions with components of the TGFβ signalling pathway. Strong genetic interactions were seen with *short gastrulation*, *crossveinless 2*, *baboon*, and the *ecdysone receptor*.

Keywords:

Huntingtin interacting protein 14, palmitoylation, Drosophila, wing development, TGFβ signalling

ACKNOWLEDGEMENTS

I would like to thank the many people who helped me with this work, just a few of whom are listed below. Michael Hayden and members of the Hayden lab: Rebecca Devon, Martina Metzler, Paul Orban, Roshni Singaraja, and especially Anat Yanai. My committee, Lynne Quarmby and Chris Beh, provided assistance and support whenever needed. Members of the Harden lab: especially Justina Sanny and Bari Zahedi. Members of the Verheyen lab especially: Wendy Lee and Arial Zeng. I would also like to thank two undergraduate students: Derk Pierik for mounting and photographing hundreds of wings and Michelle Sinden for setting up and scoring hundreds of crosses. Finally, I would like to thank Dave Baillie, Nick Harden and especially Esther Verheyen and Sheila MacLean for their patience, encouragement, and support.

TABLE OF CONTENTS

LIST OF FIGURES

LIST OF TABLES

INTRODUCTION

Huntington Disease

Huntington disease (HD) is a late onset neurodegenerative disease caused by the selective degeneration of neurons in the striatum of the basal ganglia (Bates, 2005). Those neurons affected include the medium spiny neurons that make up the majority of the striatum as well as the caudate and the putamen. The basal ganglia is a region of the brain associated with motor and learning functions, while the striatum is involved in the planning and modulation of movement.

Patients suffering from HD show a variety of symptoms including the loss of cognitive abilities (memory, attention, problem solving), changes in personality, and jerking movements of the face and body (Bates, 2005). During advanced HD these symptoms develop into dementia and chorea (almost continuous rapid, jerky, and involuntary movements). Mortality is generally due to complications of HD rather than from the disease itself (Bates, 2005).

HD is an autosomal dominant disease, which, in 1983, was mapped to the short arm of the fourth chromosome (Bates, 2005). Ten years later, the gene was identified by the Huntington's Disease Collaborative Research Group (HDCRG, 1993). The gene spans 180kb and consists of 67 exons. The *huntingtin* gene encodes a large protein (~348kD) that has a stretch of 20 to 35 glutamines (Q) near the amino-terminus. Those patients suffering from

HD had a polyglutamine (polyQ) expansion with over 40 glutamines in this region of the huntingtin protein. The number of repeats is inversely related to the age of onset. Individuals with 6-35 glutamines at the amino-terminus of the huntingtin protein are un-affected, there is increased risk in individuals with 36-39, and greater than 40 glutamines leads to fully penetrant HD. Those individuals with the most repeats are affected at the youngest age (Bates, 2005).

Max Perutz predicted that polyQ sequences could self-associate into amyloid fibrils (Perutz et al., 1993). These predicted fibrils are similar to the amyloid deposits found in all polyQ expansion diseases including HD. This polyQ expansion is a characteristic of at least nine diseases, all of which lead to late onset neurodegeneration in different subsets of neurons. The observation that each of the nine polyQ diseases affects distinct but overlapping subsets of neurons suggests the protein context of the polyQ expansion likely plays a role in the disease progression rather than the polyQ expansion itself (Morfini et al., 2005; Michael Hayden, personal communication).

Huntingtin interacting protein 14 (Hip14)

Human Hip14 was identified as a novel human huntingtin interactor in a yeast two hybrid screen (Singaraja et al., 2002). The physical interaction between Hip14 and huntingtin is dependent on huntingtin polyQ length. As polyQ length increases there is a significant reduction in binding affinity to Hip14 (Singaraja et al., 2002). Hip14 maps to the long arm of chromosome

12 (12q14-q15) though no genetic disease has been mapped to this region (Singaraja et al., 2002). Humans also have a second, Hip14-related, gene on chromosome 11 and these two proteins share 48% identity and 57% similarity (Singaraja et al., 2002). Hip14 is 633 amino acids long and contains a series of ankyrin repeats, a DHHC zinc finger domain, and six transmembrane domains. Ankyrin repeats are tandemly repeated 33 amino acid sequences and are one of the most common protein-protein interaction motifs in nature. The function of the DHHC domains was unknown at the time but has subsequently been implicated in palmitoyltransferase activity (Roth et al., 2002).

An antibody specific to amino acids 49-60 of human Hip14 detects a 73kD protein in human tissue from all regions of the brain (Singaraja et al., 2002). The highest protein levels are in the cortex, cerebellum, occipital lobe, and caudate while the lowest levels are in the spinal cord. In mouse brain sections, the highest levels of expression are detected in brain neurons from the cortex, striatum, and hippocampus (Singaraja et al., 2002). Hip14 co-localizes with huntingtin in the cytoplasmic and perinuclear regions of medium spiny neurons from the mouse striatum (Singaraja et al., 2002). Hip14 localizes to Golgi membranes and cytoplasmic vesicles (Huang et al., 2004). Together with the transmembrane topology of the yeast homolog predicted by Politis et al., 2005, this suggests that Hip14 could be involved in cytoplasmic modifications of cytoplasmic and integral membrane proteins.

Akr1p

Hip14 has sequence similarity to *Saccharomyces cerevisiae* Ankyrin repeat-containing 1 protein (Akr1p; 24% identity and 40% similarity; Kao et al., 1996). Like Hip14, Akr1p contains a series of ankyrin repeats, a DHHC zinc finger domain, and six transmembrane domains (Kao et al., 1996). The signature amino acid sequence in the DHHC domain has diverged to DHYC in Akr1p (Roth et al., 2002). Akr1p was identified in a yeast two hybrid screen using the intracellular tail of the yeast pheromone receptor sterile 3 protein (Ste3p; Givan and Sprague, 1997). Newly synthesized Ste3p is transported to the cell surface for a brief amount of time before undergoing endocytosis and degradation. Akr1p is required for this constitutive endocytosis and subsequent degradation of Ste3p (Givan and Sprague, 1997). Ste3p degradation is restored with the expression of mammalian Hip14 in *AKR1* mutants, and *AKR1* mutant temperature-sensitive defects in endocytosis can be partially rescued by Hip14 (Singaraja et al., 2002). These results suggest the Hip14 and Akr1p have a similar function.

A number of signalling molecules are tethered to the membrane through post-translational lipid modifications. One such modification, palmitoylation of cysteine residues, directs Ras and Rho, G proteins, and non-receptor tyrosine kinases to the plasma membrane (Linder and Deschenes, 2003). In *Saccharomyces cerevisiae,* palmitoylation of the Ras homolog, Ras2p, is partially defective in cells lacking "Effect on Ras function 2" protein (Erf2p), a protein containing a DHHC domain (Lobo et al., 2002).

The constitutive endocytosis of Ste3p is mediated by phosphorylation by the Yeast Casein Kinase 2 protein (Yck2p; Feng and Davis, 2000). The proper localization of Yck2p to the plasma membrane and the constitutive endocytosis of Ste3p are both dependent on Akr1p and a lipid modification of Yck2p (Feng and Davis, 2000). As Akr1p contained a DHHC domain (like Erf2p), is the localization of Yck2p due to palmitoylation by Akr1p? Both *in vitro* and *in vivo* results showed Yck2p palmitoylation was Akr1p-dependent (Roth et al., 2002). The catalytic activity of Akr1p is dependent on the DHHC domain. Changing the DHYC sequence in Akr1p to AAYC or DHYA abolished Akr1p palmitoylation activity *in vitro* (Roth et al., 2002). Furthermore, the discovery that Akr1p was also palmitoylated at the cysteine within the DHYC sequence suggested an enzymatic mechanism for Yck2p palmitoylation by Akr1p. During palmitoylation of substrate the palmitoyl-moiety of palmitoyl-CoA is transferred to Akr1p before the addition to the substrate protein. As the Yck2p palmitoylation is Akr1p dependent, catalysis requires the DHHC domain, and an enzymatic intermediate of Akr1p is itself palmitoylated this suggests that Akr1p is a Yck2p palmitoyltransferase and the DHHC may be the catalytic site.

Since all the known substrates of Akr1p are cytoplasmic it was important to confirm that the DHHC domain was cytoplasmic. A study of the transmembrane topology of Akr1p confirmed that the protein crosses the membrane bilayer six times (Politis et al., 2005). Importantly, the ankyrin repeats and DHHC domain were within the cytoplasm. This suggests a model

in which Akr1p binds substrates with the cytoplasmic ankyrin repeats before subsequent palmitoylation by the DHHC domain.

Palmitoylation

Palmitic acid is a 16-carbon fatty acid that can be post-translationally added to the sulphur atom of a cysteine residue. This modification leads to increased protein hydrophobicity and can facilitate interactions with the membrane (typically the cytosolic face of the plasma membrane) as well as alter protein sorting and function (el-Husseini and Bredt 2002). Palmitoylation is reversible *in vitro* (Camp and Hofmann, 1993) and recent evidence suggests that protein palmitoylation may be reversible *in vivo* as well (Rocks et al., 2005; Goodwin et al., 2005). There is no common palmitoylation consensus site although there are specific requirements for efficient palmitoylation such as a cysteine in close proximity to the membrane or a cysteine adjacent to a previously lipid modified amino acid. Otherwise, the cysteines are generally within a stretch of hydrophobic amino acids. Many palmitoylated cysteines are adjacent to basic residues and this may help bind acidic head groups of phosopholipids (el-Husseini and Bredt 2002).

Palmitoylation plays a number of roles in the nervous system. It has been implicated in processes from neurite outgrowth and axon pathfinding to the control of neuron transmission. At the pre-synaptic membrane, palmitoylation regulates neurotransmitter release, while palmitoylation at the post-synaptic membrane regulates signal transduction of ion channels and neurotransmitter receptors (el-Husseini and Bredt 2002). Palmitoylated

neuronal proteins include glutamate receptor 4 (GluR4), GluR6, Synaptotagmin 1, Synaptobrevin 2, synaptosomal-associated protein 25 (SNAP25), glutamic acid decarboxylase isoform 65 (GAD65), Cysteine-string protein, postsynaptic density protein 95 (PSD95; el-Husseini and Bredt 2002). Synaptotagmin I, Cysteine-string protein, and SNAP25 mediate synaptic vesicle fusion and trafficking while PSD95 palmitoylation is essential for trafficking to post-synaptic sites (el-Husseini and Bredt 2002). At the post-synaptic sites, PSD95 binds the cytoplasmic tail of NMDA receptors as well as regulating the activity of AMPA receptors to modulate synaptic strength (post-synaptic plasticity; el-Husseini and Bredt 2002).

Is Hip14 a neuronal palmitoyltransferase? Both *in vitro* and *in vivo* results indicate that Hip14 palmitoylates a number of proteins such as SNAP25, PSD95, Synaptotagmin 1, and GAD65 (Huang et al., 2004). Hip14 adds palmitate to only a specific subset of neuronal proteins, as H-Ras, lck, Paralemmin, and Synaptotagmin VII failed to be palmitoylated (Huang et al., 2004). Catalytic activity is dependent on the DHHC domain as Hip14 lacking the DHHC domain fails to palmitoylate substrates (Huang et al., 2004).

Huntingtin protein is subjected to many post-translational modifications, including palmitoylation by Hip14 (Huang et al., 2004). Palmitoylation was localized to the amino-terminus of the huntingtin protein and the site was eventually identified as C214 (a cysteine conserved in the Drosophila homolog; Yanai A et al., unpublished results). Huntingtin palmitoylation decreases as the polyQ length increases, and this is accompanied by significantly altered trafficking and intracellular localization

of huntingtin. The lack of huntingtin protein palmitoylation also accelerates protein misfolding and aggregation and leads to increased cell death (Yanai et al., unpublished results).

Pinguid

Hip14 has sequence similarity to the predicted protein encoded by the annotated gene CG6017 in Drosophila (44% identity and 59% similarity), the focus of the current study. The protein encoded by CG6017 was renamed Pinguid (derived from the Latin word pinguis: fat; oily). Like Hip14, Pinguid is predicted to contain a series of ankyrin repeats, a DHHC zinc finger domain, and six transmembrane domains.

In Drosophila, the only confirmed palmitoyltransferase is Rasp (also known as skinny hedgehog and sightless), a protein required for hedgehog activity (Chamoun et al., 2001). Hedgehog is a secreted signalling molecule that undergoes a complex series of post-translational modifications (Linder and Deschenes, 2004; Porter et al., 1996). Hedgehog is translated as a 45kD protein. Following removal of the signal sequence hedgehog undergoes intramolecular processing to yield a 20kD amino-terminal signalling fragment and a 25kD carboxyl-terminal fragment. A cholesterol is added to the carboxyl-terminal of the 20kD with the aid of the 25kD fragment; amino-terminal palmitoylation is catalyzed by rasp (Lee et al., 2001; Chamoun et al., 2001; Micchelli et al., 2002). Unlike Akr1p and Hip14, rasp contains a MBOAT (membrane bound O-acyltransferase) domain. The MBOAT domain is predicted to be oriented into the lumen of the endoplasmic reticulum in order to palmitoylate substrates (Hofmann, 2000). Another protein with an MBOAT

domain, porcupine, is required for the processing and secretion of the signalling molecule, wingless. Palmitoylation of wingless does occur but whether wingless is palmitoylated by porcupine is still unknown (Linder and Deschenes, 2004; Zhai et al., 2004).

Another two potential palmitoyltransferases in the Drosophila genome are Pinguid (CG6017) and Patsas (CG6618). Both contain a series of ankyrin repeats and a DHHC zinc finger domain. Assuming Pinguid and Patsas are palmitoyltransferases, what are their potential substrates? A yeast two hybrid screen has identified short gastrulation (sog) as a possible interactor of pinguid (Giot et al., 2003). Since sog is part of the Drosophila TGFβ signalling pathway, this information led me to study the role of pinguid in TGFβ signalling, with an emphasis on wing development.

Drosophila wing development

The adult wing (shown in Figure 1) consists of five longitudinal veins (L1 to L5), an anterior cross vein (ACV), and a posterior crossvein (PCV). The wing is formed during metamorphosis from imaginal discs in the larvae. Imaginal discs are groups of cells that (during metamorphosis) evert, elongate, and differentiate into adult structures such as the eyes, legs, and wings. Imaginal discs and the wing are frequently used to study the *dpp* signalling pathway in Drosophila. The extracellular ligand, Dpp, acts as a morphogen during wing development with the highest levels of Dpp restricted to the anterior-posterior (A-P) boundary of the wing imaginal disc (Capdevila et al., 1994). The anterior extent of dpp expression is defined by

cAMP-dependent protein kinase 1 (Pka-C1) while the posterior extent is defined by engrailed (en). Together Pka-C1 and en create a stripe of dpp expression along the A-P boundary (Sanicola et al., 1995). Following metamorphosis the A-P boundary corresponds to the centre of the L3-L4 intervein region (Figure 1). Following secretion by the stripe of cells along the A-P boundary, Dpp diffuses in the anterior and posterior directions. The concentration gradient of Dpp detected by cells in the wing imaginal disc directs distinct outputs as a function of distance from the Dpp source (the A-P boundary; Nellen et al., 1996). The development of L3, L4, and the intervein region are dependent on Dpp signalling activity. Genetic modifications can increase or decrease the range of the Dpp concentration gradient and result in increased or decreased intervein tissue in the adult wing. For example the ectopic expression of high levels of the type I TGFβ receptor thick veins (Tkv) along the A-P boundary results in binding to Dpp and limits the diffusion of Dpp leading to complete loss of L3-L4 intervein tissue (Lecuit and Cohen, 1998).

Figure 1 – Adult wing. The adult wing consists of five longitudinal veins (labelled L1 to L5), an anterior crossvein (ACV), and a posterior crossvein (PCV).

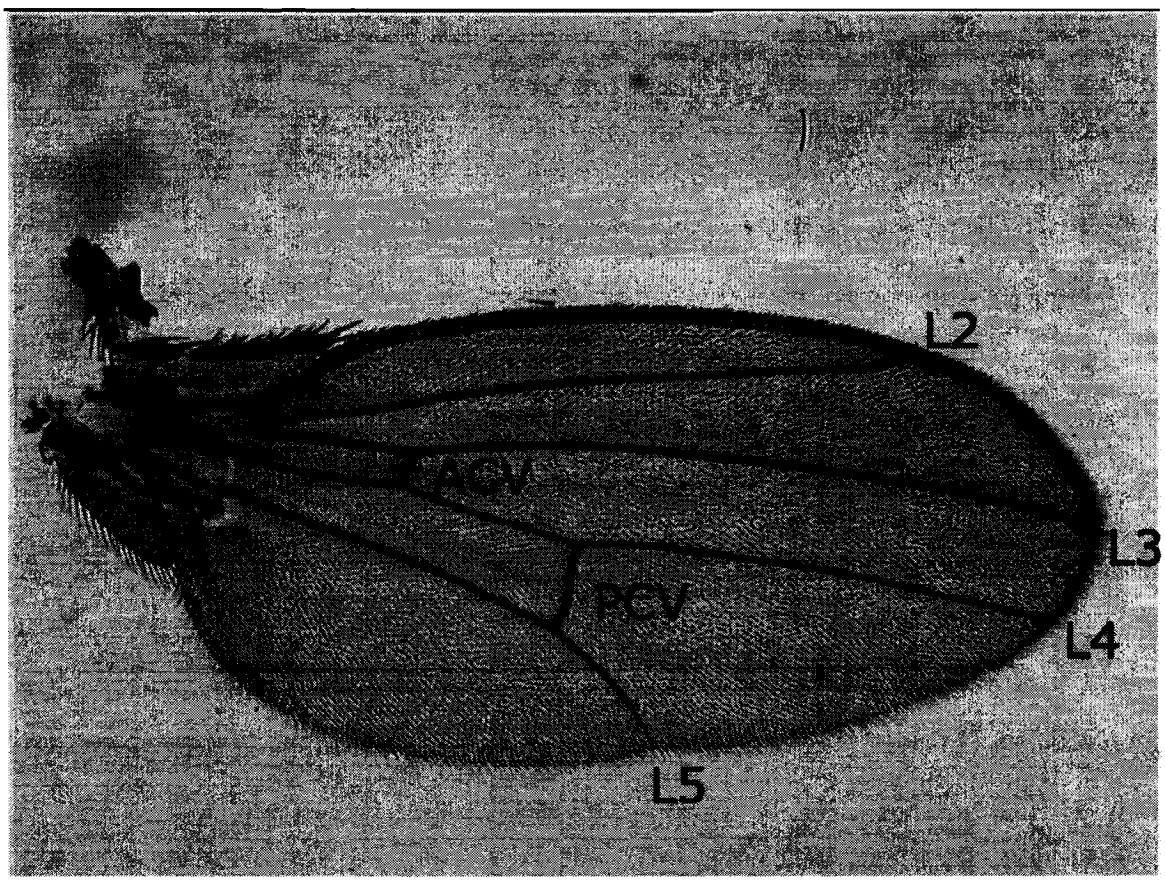

TGFβ signalling

The transforming growth factor β (TGFβ) signalling pathway is conserved in vertebrates and invertebrates; a number of Drosophila genes involved in the pathway are listed in Table 1. There are three classes of TGFβ signalling: activin, bone morphogenetic protein (BMP), and TGFβ. In Drosophila Dpp, Gbb, and Scw are all BMPs (see abbreviations in Table 1). The pathway proceeds as follows (Raftery and Sutherland, 1999): TGFβ, an extracellular ligand, binds to the TGFβ receptor. The receptor consists of one type I serine/threonine kinase (Tkv or Babo) and one type II serine/threonine kinase (Put, Sax, or Wit). Both of these receptors consist of an extracellular domain that bind ligand, a single transmembrane domain, and an intracellular kinase domain. Formation of the ligand-induced receptor complex allows the constitutively active kinase activity on the type II receptor to phosphorylate and activate the type I receptor. SARA (Tsukazaki et al., 1998) aids in recruiting receptor regulated Smad (R-Smad; Mad or dSmad2) to the type I receptor where the R-Smad is phosphorylated by the type I receptor. Once activated, the R-Smad forms a complex with a common mediator Smad (Co-Smad; Med) and translocates to the nucleus. In the nucleus, Smads positively or negatively regulate transcription by recruiting co-activators or co-repressors to the promoter.

Table 1 – Drosophila genes involved in TGFβ signalling.

Extracellular regulators of TGFβ		
crossveinless 2	cv-2	positive regulator
short gastrulation	sog	negative regulator
TGFβ Ligands		
activin-β	act-β	
decapentaplegic	dpp	
glass bottom boat	gbb	
screw	scw	
TGFβ Receptors		
baboon	babo	Type I receptor
punt	put	Type II receptor
saxophone	sax	Type II receptor
thickveins	tkv	Type I receptor
wishful thinking	wit	Type II receptor
Smads		
Mothers against dpp	Mad	R-Smad
Medea	Medea	Co-Smad
Smad on X	dSmad2	R-Smad
Others		
Smad anchor for receptor activation	SARA	
spalt major	salm	target gene
optomotor blind	omb	target gene
vestigial	vg	target gene
Ecdysone receptor	EcR	target gene

TGFβ signalling in Drosophila wing development

Patterning of the wing imaginal disc and the adult wing is regulated by Dpp signalling (Figure 2). In the developing wing, Dpp is negatively regulated by Sog (short gastrulation) and positively regulated by Crossveinless 2 (Cv-2). Sog and Cv-2 are both extracellular proteins that prevent or potentiate Dpp diffusion (Eldar et al., 2002; Conley et al., 2000). The Dpp receptor consists of one type I serine/threonine kinase (Tkv) and one type II serine/threonine kinase (Put). Formation of the Dpp-induced receptor complex allows the constitutively active Put to phosphorylate and activate Tkv. Activated Tkv then goes on to phosphorylate Mad. Once activated, Mad forms a complex with Med which translocates to the nucleus. In the nucleus the Mad/Med complex leads to transcription of a number of genes including *salm*, *omb*, and *vg*.

Figure 2 – TGFβ signalling in Drosophila. (A) In Dpp signalling Dpp is negatively regulated by Sog and positively regulated by Cv-2. Dpp binds to Tkv and Put (1). Formation of the Dpp-induced receptor complex (2) allows the constitutively active Put to phosphorylate and activate Tkv (3). Activated Tkv then goes on to phosphorylate Mad (4). Once activated, Mad forms a complex with Med which translocates to the nucleus. In the nucleus the Mad/Med complex leads to transcription of a number of genes including *salm*, *omb*, and *vg*. (B) In Activin signalling the diffusion or activity of the ligand, Act-β, is likely regulated by extracellular proteins. Act-β binds to Babo and Wit (1). Formation of the Act-β-induced receptor complex (2) allows the constitutively active Wit to phosphorylate and activate Babo (3). dSmad2 is recruited to the receptor complex by SARA where Babo goes on to phosphorylate dSmad2 (4). Once activated, dSmad2 is thought to form a complex with a Co-Smad and translocate to the nucleus.

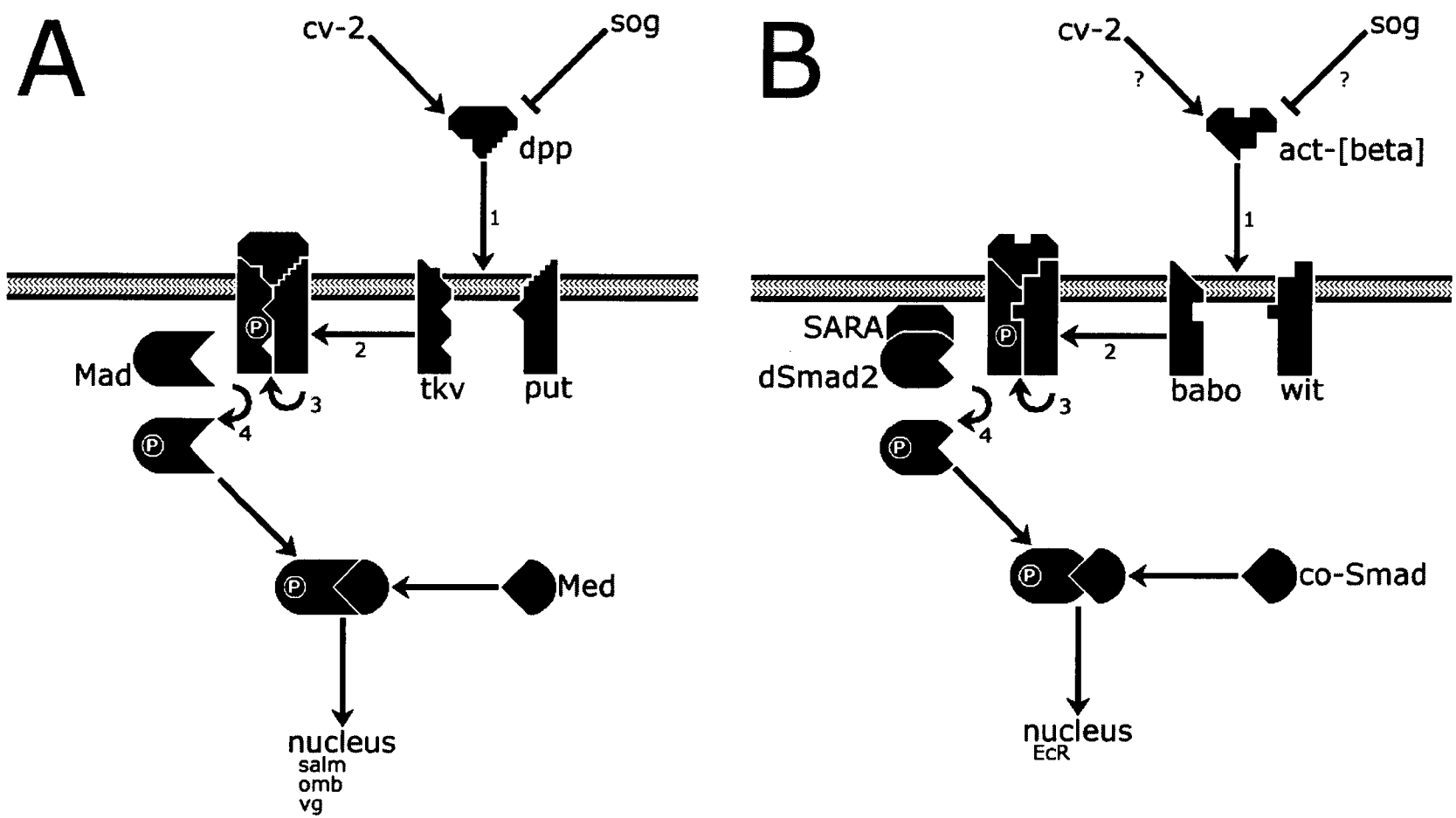
A
cv-2
sog
dpp
1
Mad
2
tkv
put
3
4
Med
nucleus
salm
omb
vg
B
cv-2
sog
?
?
act-[beta]
1
SARA
dSmad2
2
babo
wit
3
4
co-Smad
nucleus
EcR

Cell proliferation in the Drosophila imaginal discs appears to be regulated by Activin signalling. In the Drosophila wing over-expression of constitutively activated Babo leads to an adult wing that is approximately 30% larger than wildtype due to a larger number of cells (rather than bigger cells; Brummel et al., 1999). While Babo is essential for metamorphosis, the gene is not required during embryogenesis. The major defect seen in *babo* mutants is a reduction of cell proliferation in imaginal discs (Brummel et al., 1999). Any wings that are recovered from *babo* mutants are dramatically reduced in size but have only minor patterning defects (Brummel et al., 1999). Over-expression of dSmad2 also leads to a larger wing: approximately 20% larger than wildtype (Marquez et al., 2001). Both Babo and dSmad2 are required for remodelling neurons during metamorphosis (Zheng et al., 2003).

The Activin signalling pathway is not as well studied as the Dpp pathway. (Figure 2). The diffusion or activity of the ligand, Act-β, is likely regulated by extracellular proteins (much like Dpp) but none have been identified so far. The Act-β receptor consists of one type I serine/threonine kinase (Babo) and one type II serine/threonine kinase (Wit). Formation of the Act-β-induced receptor complex allows the constitutively active Wit to phosphorylate and activate Babo. SARA may aid in recruiting dSmad2 to the receptor complex where dSmad2 is phosphorylated by Babo (Bennett and Alphey, 2002; Brummel et al., 1999). Once activated, dSmad2 is thought to form a complex with a Co-Smad (potentially Med) and translocate to the

nucleus. So far, *EcR* is the only known gene whose transcription is known to be regulated by dSmad2 (Zheng et al., 2003).

EcR is the receptor for the Drosophila steroid hormone 20-hydroxyecdysone (ecdysone). Pulses of ecdysone direct Drosophila development throughout its lifecycle (Thummel, 1995). Peak hormone levels direct the organism through the three stages of larval development as well as providing a signal to initiate metamorphosis. In addition to the transformation of a larva to an adult, neurons are remodelled during morphogenesis and this neuronal plasticity appears to be regulated by TGFβ signalling (Zheng et al., 2003).

This study looks at the possible role of *pinguid* in TGFβ signalling. To study *pinguid in vivo,* I have generated mutants and also over-expressed the gene in an attempt to determine *pinguid's* function in Drosophila. Although *pinguid* encodes an essential protein, its role in development has remained elusive. Two pieces of evidence suggest a role in TGFβ signalling: wing phenotypes reminiscent of TGFβ signalling mutants are observed when pinguid is over-expressed, and pinguid genetically interacts with several known members of the TGFβ signalling pathway. Since *pinguid*, the Drosophila homolog of Hip14, is predicted to encode a palmitoyltransferase, this could mean that regulation of the TGFβ signalling pathway involves palmitoylation.

RESULTS

Identification of the Drosophila Hip14 homolog

In an effort to begin to elucidate the cellular function of Hip14, a genetic approach using Drosophila was initiated. The FlyBase BLAST Service identified CG6017 in *Drosophila melanogaster* as the closest Drosophila homolog to human Huntingtin-interacting protein 14 (Q8IUH5). CG6017 has 44% identity and 59% similarity to Hip14 (Figure 3) while the next closest protein is CG6618 (22% identity and 37% similarity). CG6017 (renamed *pinguid*) is located at 72C1 on the left arm of the third chromosome proximal to *brahma*, *Arflike at 72A*, and *DNA-polymerase-δ* (Tamkun et al., 1991; Tamkun et al., 1992; Chiang and Lehman, 1995). The gene is approximately 3.4 kb long and encodes a protein of 637 amino acids.

Figure 3 – Protein sequence alignment of Hip14 and homologs. Alignment of pinguid (Dm, AAF49554), Drosophila pseudoobscura (Dp, EAL30521), Homo sapiens (Hs, Q8IUH5), and Mus musculus (Mm, Q80TN5). The six conserved ankyrin repeats are outlined by the double line, the DHHC zinc finger domain is outlined by the bold line, and the six transmembrane regions are indicated in bold. Identical and conserved amino acids are highlighted in light grey; dark grey indicates the DHHC sequence.

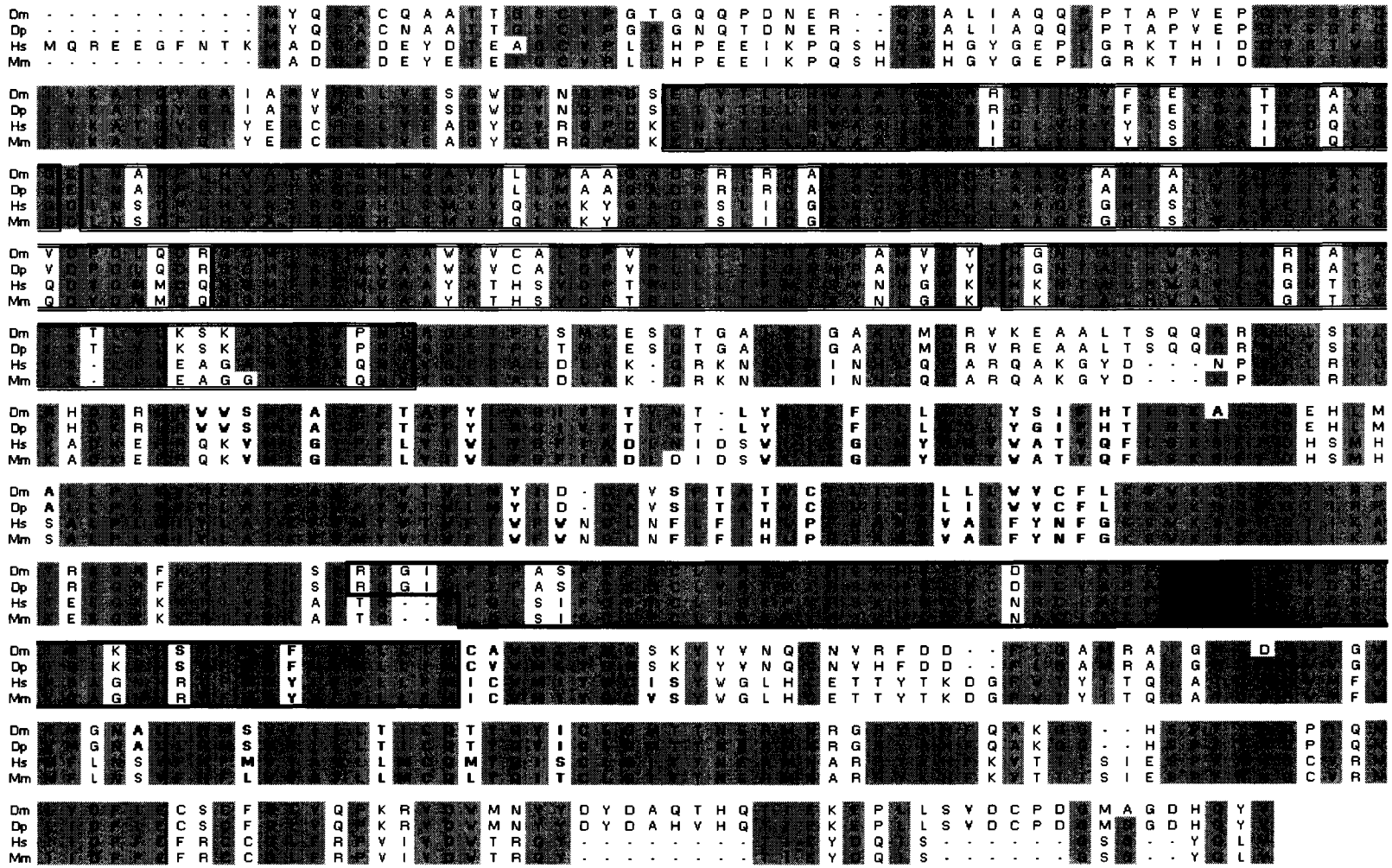
Dm
Dp
Hs
Mm

Several Drosophila stocks are available that contain large genomic deletions that include 72C1. These deletions are all homozygous lethal and are maintained as heterozygous stocks with a balancer chromosome. Balancer chromosomes contain multiple inversions within the same chromosome (to prevent recombination), several dominant markers (for identification of the chromosome), a number of recessive markers, and are lethal as homozygotes. One of these deletion stocks, *Df(3L)brm11*, is very well characterized. This ~240 kb deficiency contains 31 predicted genes and has been used to screen for ethyl methane sulphonate (EMS)-induced alleles of two genes in the region: *cAMP-dependent protein kinase* (Melendez et al., 1995) and *brahma* (Brizuela et al., 1994). Also located in the vicinity are two P-element insertions that could be used for P-element mediated excision of the *pinguid* locus when a source of transposase is available.

A homozygous viable P-element insertion (EP3292; Rorth et al., 1996) is located within the 5′ un-translated region (UTR) of *DNA-polymerase-δ* and 55 bp 5′ to the predicted start codon of *DNA-polymerase-δ* (Figure 4). This P-element insertion contains the *white* gene as well as an upstream activating sequence (UAS) for GAL4 directed over-expression of the flanking genomic DNA in the direction of CG6017. This insertion had previously been used to identify CG6017 as a gene controlling embryonic motor axon guidance and synaptogenesis when CG6017 was over-expressed using EP3292 under the control of the neuron-specific Gal4 driver c155 (elav; Kraut et al., 2001).

Figure 4 – P-element map. Map indicating the location of EP3292 and EY09853 in relation to *DNA-polymerase-δ* and *pinguid*. EP3292 contains the *white* gene and has a UAS sequence at the 3′ end. EY09853 contains the *yellow* and *white* genes and has a UAS sequence at the 5′ end. To the left of *DNA-polymerase-δ* (in the direction of the telomere) is *Arflike at 72A*. To the right of *pinguid* (in the direction of the centromere) is *CG5830*.

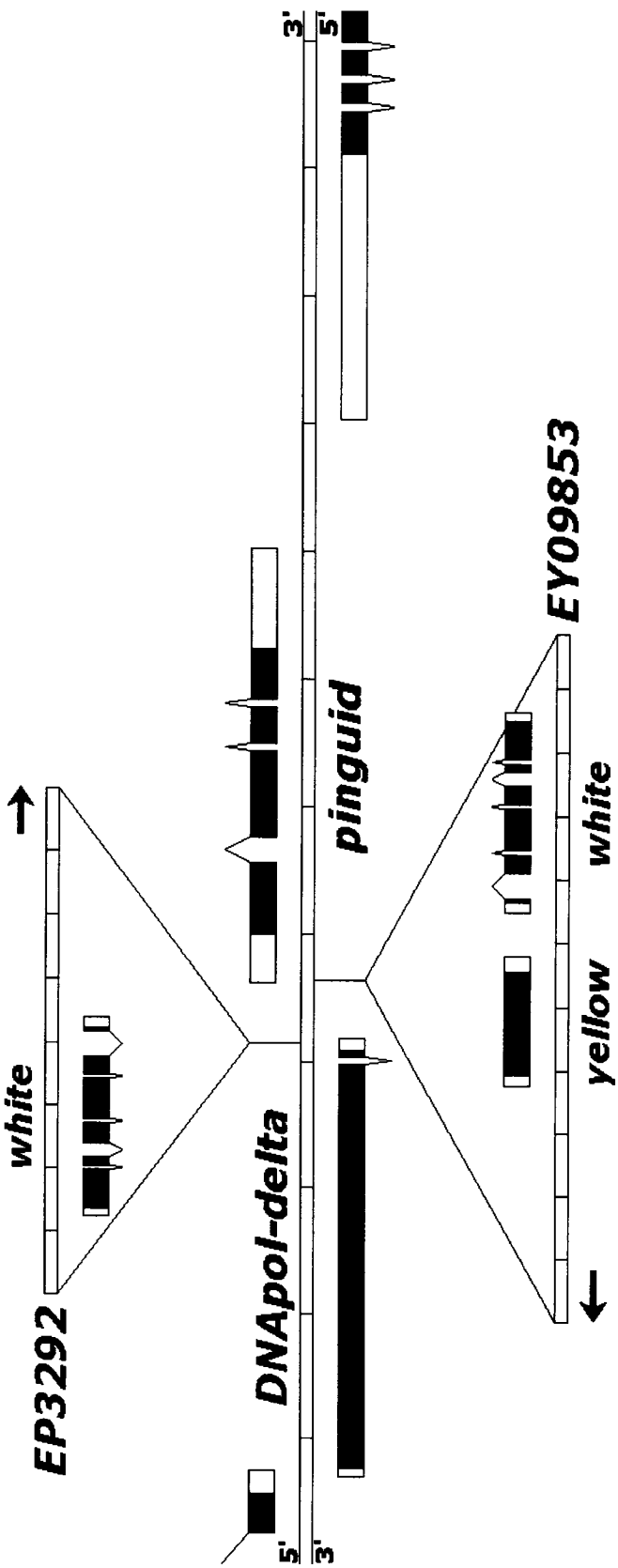
3'
5'
pinguid
EY09853
white
yellow
white
EP3292
DNApol-delta
5'
3'

Another homozygous viable P-element insertion (EY09853; Bellen et al., 2004) is located within the 5′ UTR and 360bp 5′ to the predicted start codon for *pinguid* (Figure 4). This P-element insertion contains the *yellow* and *white* genes as well as UAS sequences for GAL4 directed over-expression of the flanking genomic DNA (incorrect orientation for *pinguid* over-expression).

pinguid P-element excision screen

Two P-element excision screens were carried out using these insertion lines. Transposase mediated P-element excision can result in several outcomes: (1) the P-element may excise precisely, restoring the genomic DNA to wildtype; (2) the P-element may hop to another location in the genome; (3) the P-element may lose internal sequences leaving the genomic DNA unaffected; or (4) the P-element may imprecisely excise, taking flanking genomic DNA in the process. To create deletions of the *pinguid* locus, a P-element screen was undertaken to isolate imprecise excisions.

Individuals lacking the *white* gene were selected in the EP screen to indicate that the P-element was excised. In the EPgy2 screen I looked for individuals lacking the *yellow* and/or *white* genes. I looked at 42 individual excision events from the EP screen. Twenty-four of these were homozygous viable and were rejected by PCR analysis, as the *DNA-polymerase-δ* and *pinguid* loci were unaffected. Of the remaining lethal excision events, 13 were viable in combination with *Df(3L)brm11* indicating that lethality was not due to a mutation in the region of interest. These 13 were discarded and the

remaining five lethal excisions were crossed to the nine EMS induced alleles that map to *Df(3L)brm11*. Of these, the excisions were lethal with *l(3)72Ac*^{I10} and/or *l(3)72Ad*^{I25}. Further complementation tests (Table 2) and PCR confirmed that *l(3)72Ac*^{I10} was a *DNA-polymerase-δ* allele and *l(3)72Ad*^{I25} was a *pinguid* allele. The two excision alleles of *DNA-polymerase-δ* were renamed *DNApol-delta*^{X1} and *DNApol-delta*^{X2}. Two more *l(3)72Ac* EMS induced alleles were obtained from Daniel Kalderon (Columbia University) and the three EMS induced alleles were renamed *DNApol-delta*^{I10}, *DNApol-delta*^{I13}, and *DNApol-delta*^{J10}.

For the EPgy2 screen, 171 individual excision events were scored. 131 of these were homozygous viable and were rejected by PCR analysis, as the *DNA-polymerase-δ* and *pinguid* loci were unaffected. Of the remaining lethal excision events, 31 were viable in combination with *Df(3L)brm11* and discarded (lethality was not due to a mutation in the region of interest). The remaining nine lethal excisions were crossed to the nine EMS induced alleles that map to *Df(3L)brm11*. All nine excisions were lethal with *l(3)72Ac*^{I10} and/or *l(3)72Ad*^{I25}. Further complementation tests (Table 2) and PCR analysis confirmed that *l(3)72Ac*^{I10} was a *DNA-polymerase-δ* allele and *l(3)72Ad*^{I25} was a *pinguid* (*ping*) allele. Three of the excisions were alleles of *pinguid* alone and were renamed *ping*^{X1}, *ping*^{X2}, and *ping*^{X3}. One more *l(3)72Ad* EMS allele was obtained from Daniel Kalderon and the two EMS induced alleles were renamed *ping*^{I25} and *ping*^{K8}.

Table 2 – Complementation tests. Lethal EP3292 and EY09853 excisions events (original names) were crossed to two deficiencies, nine EMS mutants in the region, and to each other. *EP0306D* was renamed *DNApol-delta*^{X1}, *EP0315X* renamed *DNApol-delta*^{X2}, *EY1207A* was renamed *pinguid*^{X1}, *EY1213K* was renamed *pinguid*^{X2}, and *EY0227E* was renamed *pinguid*^{X3}. For each cross a "V" indicates that the progeny of the cross were homozygous viable while an "L" indicates that the progeny were homozygous lethal.

	Df(3L)brm11	Df(3L)XG5	EP0306D	EP0315A	EP0315X	EP0315Y	EP0408S	EP3292	EY1207A	EY1210F	EY1213K	EY1214F	EY1216A	EY0225B	EY0227E	EY09853
Df(3L)brm11	L		L	L	L	L	L	V	L	L	L	L		L	L	V
Df(3L)XG5		L	L		L						L			L	L	
Arf72A		L	V	V	V	V	V	V	V	V	V	V	L	V	V	V
l(3)72Ab			V	V	V	V	V		V	V	V	V	V		V	V
l(3)72Ac[I10]	L	L	L	L	L	L	L	V	V	L	V	L	L	L	V	V
l(3)72Ac[I13]	L	L														
l(3)72Ac[J10]	L	L														
l(3)72Ad[I25]	L	L	V	L	V	L	L	V	L	V	L	L	L	L	L	V
l(3)72Ad[K8]	L	L						V	L		L			L	L	
l(3)72CDa		L	V	V	V	V	V	V	V	V	V	V	V	V	V	
l(3)72CDb		V	V	V	V	V	V		V	V	V	V		V	V	
l(3)72CDc		L	V	V	L	V	V	V	V	V	V	V	L	V	V	V
l(3)72CDd		L	V	V	V	V	V	V	V	V	V	V		V	V	V
l(3)72CDe		V	V	V	V	V	V	V	V	V	V		V	V	V	V
EP0306D	-	-	L	L	L	L	L	L	V	L	V	L	L			V
EP0315A	-	-	-	L	L	L	L	L	L	L	L	L	L			V
EP0315X	-	-	-	-	L	L	L		V	L	V	L	L			
EP0315Y	-	-	-	-	-	L	L		L	L	L					
EP0408S	-	-	-	-	-	-	L		L	L	L	L	L			V
EP3292	-	-	-	-	-	-	-	L	V	V	V					
EY1207A	-	-	-	-	-	-	-	-	L	V	L	L	L			V
EY1210F	-	-	-	-	-	-	-	-	-	L	V	L	L			V
EY1213K	-	-	-	-	-	-	-	-	-	-	L		L			
EY1214F	-	-	-	-	-	-	-	-	-	-	-	L				
EY1216A	-	-	-	-	-	-	-	-	-	-	-	-	L			
EY0225B	-	-	-	-	-	-	-	-	-	-	-	-	-	L		
EY0227E	-	-	-	-	-	-	-	-	-	-	-	-	-	-	L	
EY09853	-	-	-	-	-	-	-	-	-	-	-	-	-	-	-	V

The *ping*^{X1} allele is a homozygous lethal *pinguid* allele generated by imprecise P-element excision and the loss of the *yellow* and *white* markers. The primer annealing sites for PCR primers 3528-F, 4032-F, 4197-F, and 4465-F are still present 5′ to the EY09853 insertion site (primer locations shown in Figure 12). On the 3′ side of the insertion site 4936-F and 5169-R are not present. A 1.3 kb PCR product is amplified from template DNA isolated from *ping*^{X1} mutants using 3528-F and 5911-R (Figure 5). As the wildtype PCR product is 2.4 kb this suggests that the deletion is approximately 1.1 kb. Sequencing of the PCR product confirms a deletion of 1197 bp from the EY09853 insertion site in the direction of *pinguid* (14bp of p-element sequence remain at the site of insertion). If the protein were still translated the predicted protein would be missing the first 267 amino acids (all the five predicted ankyrin repeats). Since the 5′UTR and the start codon are missing it is more likely that translation does not occur, thus no protein would be produced, and this allele is a null mutation.

Figure 5 – PCR across P-element excisions. PCR products amplified from *ping*^{X1}, *ping*^{X3}, control DNA, and no DNA using 3528-F and 5911-R. A 2.4 kb PCR product is amplified from control DNA.

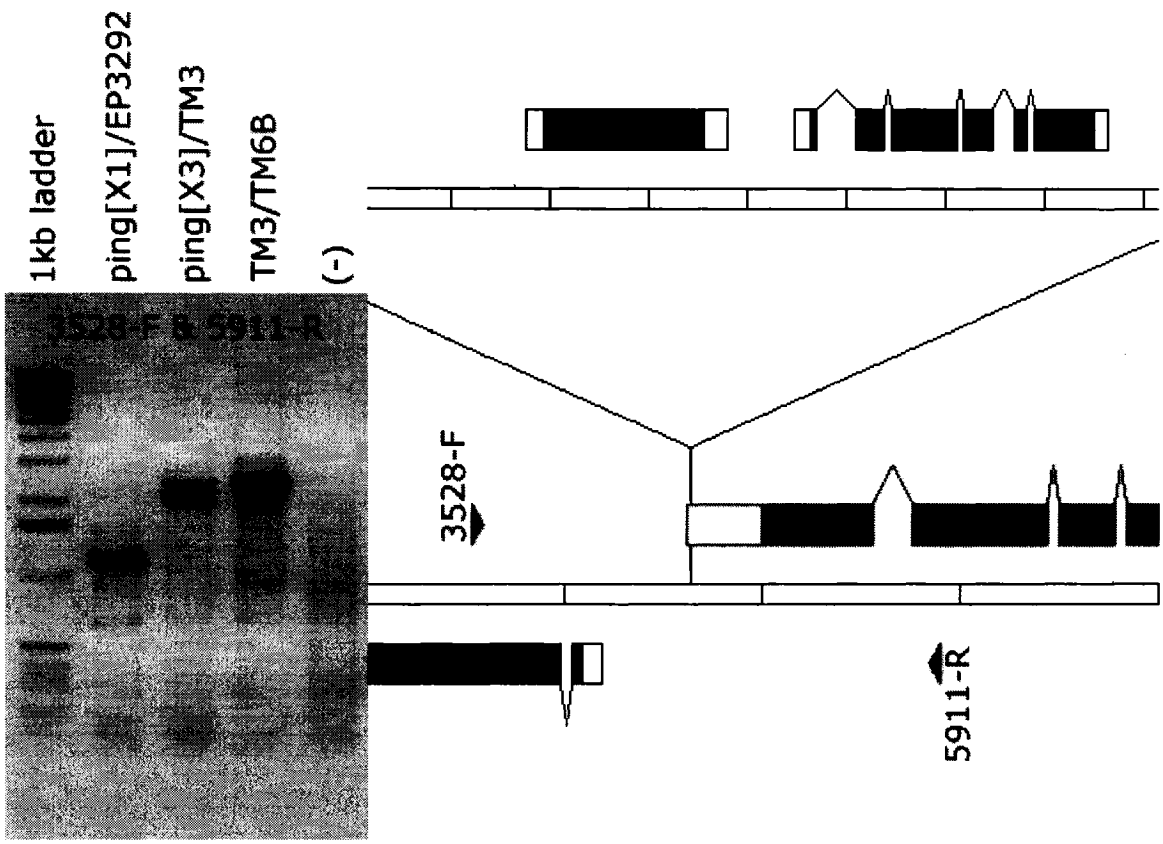

The *ping*^{X2} allele is a homozygous lethal *pinguid* allele generated by potential imprecise P-element excision and the loss of the *white* marker (the yellow maker remains). Using template DNA isolated from the original EY09853 stock, a 6 kb PCR product was amplified using the yellow-F and 5169-R primers while a 4 kb PCR product was amplified using the yellow-F and white-R primers. No PCR products were obtained using template DNA isolated from *ping*^{X2} mutants as described for the EY09853 template DNA. All other attempts to generate a PCR product from within the *yellow* gene into genomic DNA have been unsuccessful so it is unclear how far the deletion extends or whether a deletion exists.

The *ping*^{X3} allele is a homozygous lethal *pinguid* allele generated by imprecise P-element excision and the loss of the *yellow* and *white* markers. The primer annealing sites for 3528-F, 4032-F, 4197-F, and 4465-F are still present 5′ to the EY09853 insertion site. On the 3′ side of the insertion site 4936-F is not present (Figure 12). A 2.0 kb PCR product is amplified from template DNA isolated from *ping*^{X3} mutants using 3528-F and 5911-R (Figure 5). As the wildtype PCR product is 2.4 kb this suggests that the deletion is approximately 0.4 kb. Sequencing of the PCR product confirms a deletion of 371 bp from the EY09853 insertion site in the direction of *pinguid* (16bp of p-element sequence remain at the site of insertion). If the protein were still translated the predicted protein would only be missing the first 7 amino acids. Since the 5′UTR and the start codon are missing it is more likely that translation does not occur, thus no protein would be produced, and this allele is a null mutation.

Analysis of the mutants

In an effort to determine the function of *pinguid*, the mutant alleles were characterized more fully. The *pinguid* mutants have no obvious defects in morphology or patterning. As the EP3292 insertion had been used previously to identify CG6017 as a gene controlling embryonic motor axon guidance and synaptogenesis and HD affects the CNS, the staining pattern of neuronally-expressed proteins was examined in the embryonic central nervous system using the BP102 antibody. Examination of embryos revealed no differences between $ping^{I25}$, $ping^{K8}$, and wildtype embryos (Figure 6). Although the CNS looks normal, this does not preclude more subtle defects or defects in synaptic activity such as receptor trafficking and endocytosis. $ping^{X1}$ and $ping^{X3}$ die at some point during the early larval period as very few of these homozygous larvae are seen, although the embryos appear to hatch (using the TM6B, Tb^1 balancer chromosome). Homozygous $ping^{X2}$ mutants reach the pharate adult stage (fully developed adults that fail to eclose from their pupal cases) but, when dissected out of their pupal cases, showed no obvious defects, and both wings and eyes appeared normal.

Figure 6 – BP102 staining in wildtype and mutant embryos. Antibody staining of the embryonic ventral nerve cord using BP102. Ventral view of (A) w^{1118}, (C) $ping^{I25}$ and (E) $ping^{K8}$ with anterior to the left. Side view of (B) w^{1118}, (D) $ping^{I25}$ and (F) $ping^{K8}$ with anterior to the left and dorsal up.

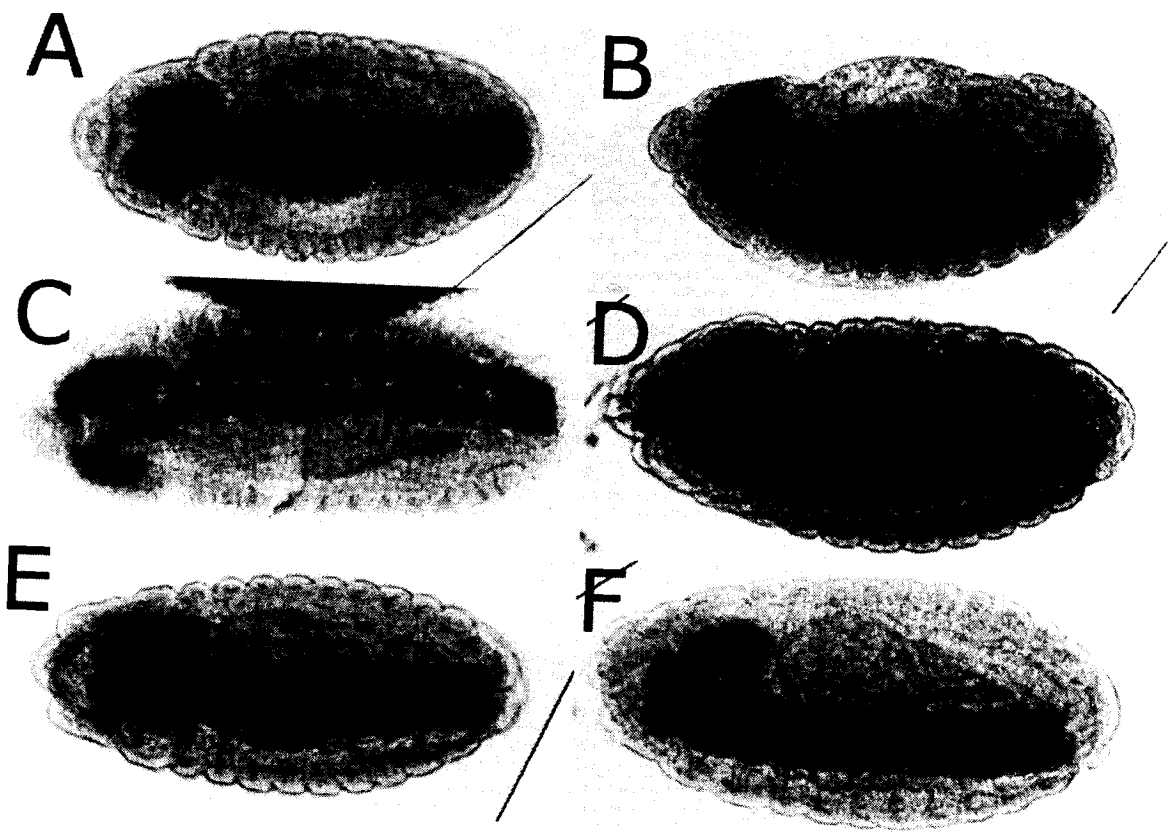

Over-expression of pinguid

To parallel the characterization of the loss-of-function mutant generated by the P-element excision, an ectopic expression approach was initiated to glean more information on *pinguid* function. A *pinguid* cDNA was cloned into pP{UAST} and injected into w^{1118} embryos to create *UAS-pinguid* transgenic fly strains. Two strains were isolated: one contained a *UAS-pinguid* insertion on the second chromosome and another on the third chromosome. To induce transcription of the *UAS-pinguid*, these transgenic lines were crossed to a number of Gal4 drivers that express the Gal4 transcriptional activator during different stages and in different tissues (Brand and Perrimon, 1993).

A number of wing Gal4 drivers generated interesting phenotypes (Figure 7). *69B-Gal4* is expressed through the wing imaginal disc (Brand and Perrimon, 1993; Staehling-Hampton et al., 1994). Expressing *pinguid* with this Gal4 driver results in a severe reduction of wing tissue but, while the longitudinal vein appear intact, the crossveins are severely reduced (Figure 7B). The *apterous-Gal4* (*ap*) driver strongly expresses on the dorsal region of the wing disc (Marquez et al., 2001). Adults expressing *pinguid* under the control of this Gal4 driver are rare. Those adults that do eclose have a very severe wing phenotype (Figure 7C). Some longitudinal vein tissue is visible in these wings but the blisters that are also present obscure most of the veins. The expression of *pinguid* using *engrailed-Gal4* (*en*) is restricted to the posterior half of the imaginal disc. In these wings there is a reduction of wing tissue, partial loss of the ACV and L5, and complete loss of the PCV (Figure

7D). Gal4 is expressed in a stripe of cells along the A-P boundary (between L3 and L4) using *patched-Gal4* (*ptc*; Sun and Artavanis-Tsakonas, 1997; Marquez et al., 2001). Expression of *pinguid* with this Gal4 driver results in a mild phenotype: the L3-L4 intervein region is reduced by approximately 20% and the ACV is missing (Figure 7E). Using the *scalloped-Gal4* driver (*sd*) to express *pinguid* throughout wing development results in a phenotype similar to that seen with *69B-Gal4*. There is a severe reduction of wing tissue but, as opposed to *69B-Gal4*, the ACV is intact (Figure 7F).

Figure 7 – Gal4 over-expression of pinguid in the wing. (A) w^{1118}, (B) *69B-Gal4>UAS-pinguid*, (C) *ap-Gal4>UAS-pinguid*, (D) *en-Gal4>UAS-pinguid*, (E) *ptc-Gal4>UAS-pinguid*, and (F) *sd-Gal4>UAS-pinguid*.

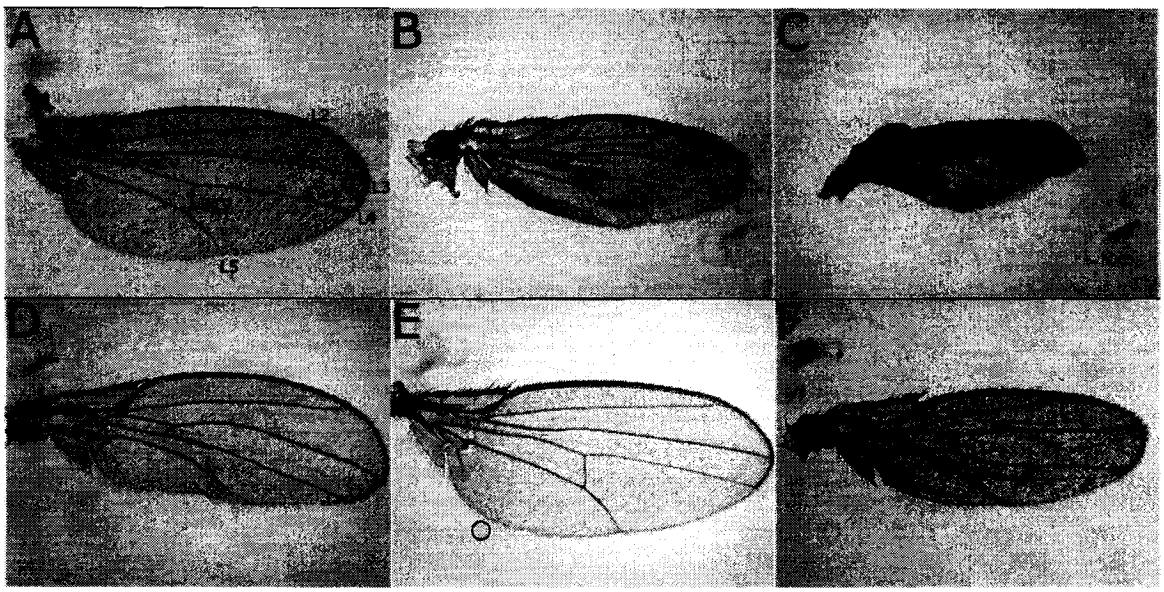

Because *ptc-Gal4>UAS-pinguid* produced a consistent defect in wing patterning and these flies were healthy, *ptc-Gal4* was recombined onto the second chromosome with *UAS-pinguid*. Five recombinant lines were established and used to study genetic interactions with a variety of mutants to determine whether other genes could enhance or suppress the *ptc-Gal4>UAS-pinguid* wing patterning defect. To quantitate wing pattern defects the distance between longitudinal veins three (L3) and L4 at the posterior crossvein (PCV) were measured as a fraction of the distance between L3 and L5 at the PCV (Figure 8). The average distance, number of samples, and the probability of the means being significantly different is stated in parenthesis.

As a control for genetic interactions with mutants the *ptc-Gal4>UAS-pinguid* recombinants were crossed to w^{1118} (Table 3). Wings from the progeny were collected and measured; the L3-L4/L3-L5 fraction at the PCV is 0.421 (n = 45). This distance is approximately 20% smaller than wildtype and is statistically significant. In a wildtype wing the L3-L4/L3-L5 fraction at the PCV is 0.526 (n = 8, p = 0.000). As a control for genetic interactions with UAS-constructs the *ptc-Gal4, UAS-pinguid* recombinants were crossed to UAS-lacZ. Wings from the progeny were collected and measured; the L3-L4/L3-L5 fraction at the PCV is 0.441 (n = 17). This distance is approximately 15% smaller than wildtype and is statistically significant (average = 0.526, n = 8, p = 0.000).

Figure 8 – Wing measurements. (A) w^{1118} with the veins labelled and then examples of *ptc-Gal4, UAS-pinguid* crossed to (B) w^{1118}, (C) *UAS-lacZ*, and (D) *Df(3L)H99*.

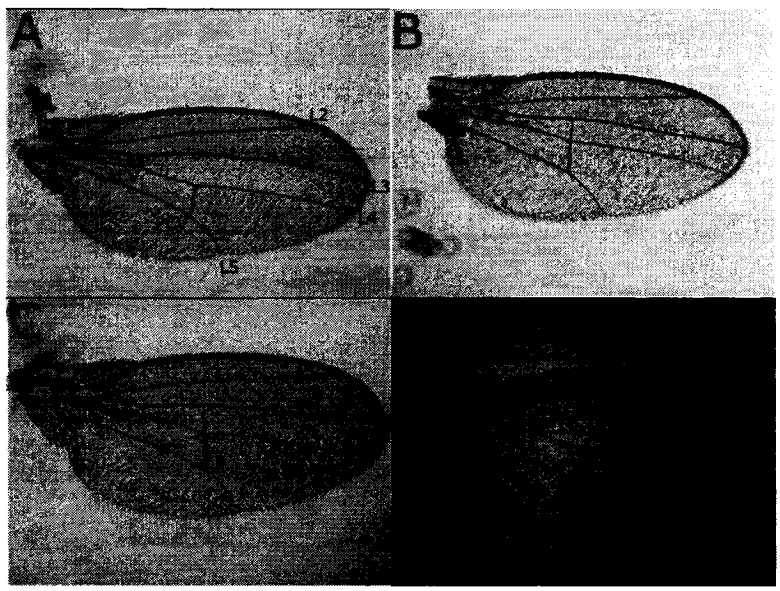

The reduction of tissue between L3 and L4 seen in the *ptc-Gal4>UAS-pinguid* wings could be due to apoptosis. If apoptosis is leading to the reduction of intervein tissue removing genes involved in apoptosis could suppress the wing phenotype. Three genes involved in Drosophila apoptosis (*grim*, *reaper*, and *head involution defective*) are clustered together on the third chromosome and a deletion stock, *Df(3L)H99*, is commonly used to suppress apoptosis. As the *ptc-Gal4>UAS-pinguid* wing phenotype is unaffected by the addition of *Df(3L)H99* (average = 0.436, n = 8, p = 0.131) it appears that the reduction in L3-L4 intervein tissue is not due to apoptosis (Figure 8 and Table 3).

Table 3 – Wing measurements.

		average	count	p-value
L3-L4/L3-L5 fraction at the PCV in a wildtype wing		0.526	8	0.000
ptc-Gal4 > UAS-pinguid crossed to:				
w[1118]	*white*	0.421	45	-
UAS-lacZ	*UAS-lacZ*	0.441	17	-
Df(3L)H99	*grim, reaper, head involution defective*	0.436	8	0.131

Pinguid's role in TGFβ signalling

The reduction of tissue between L3 and L4 seen in the *ptc-Gal4>UAS-pinguid* wings was reminiscent of, but less severe than, over-expression of Tkv with *ptc-Gal4* (Sosu-Sedzorme et al., unpublished results). In *ptc-Gal4>UAS-tkv* wings L3 and L4 are fused and the intervein tissue is absent. If the *ptc-Gal4>UAS-pinguid* wing phenotype is due to reduced TGFβ signalling the addition of TGFβ signalling mutants into the *ptc-Gal4>UAS-pinguid* background should enhance or suppress the wing phenotype depending on a genes positive or negative role in regulating TGFβ signalling (Figure 9).

In the developing wing, *dpp* is negatively regulated by *sog* and positively regulated by *cv-2*. Over-expression of *UAS-sog* (Figure 9P) within the *ptc-Gal4>UAS-pinguid* background resulted in a moderate suppression as compared to the *UAS-lacZ* control (Figure 9B, p = 0.000). One *cv-2* allele ($cv\text{-}2^{1}$) was visibly able to suppress the wing phenotype (Figure 9D, p = 0.000) while another allele ($cv\text{-}2^{225\text{-}3}$) slightly but statistically suppressed the wing phenotype (p = 0.002). The other alleles tested are shown in Table 4. Although these results suggest a role for *pinguid* in TGFβ signalling the results were the opposite of what may have been expected. If *dpp* signalling activity is already reduced, the over-expression of a negative regulator of TGFβ signalling activity or removing a positive regulator of TGFβ signalling activity should enhance the wing phenotype. These results suggest that

pinguid may be enhancing TGFβ signalling activity rather than reducing the activity.

Alleles of several TGFβ signalling ligands statistically suppressed the wing phenotype. This included three of the four *dpp* alleles tested, one of the two *gbb* alleles, one of the two *scw* alleles (an embryo specific BMP), and an *activin-β* allele (Table 4). As with the *sog* and *cv-2* results, these results suggest that *pinguid* is enhancing TGFβ signalling activity.

Table 4 – Extracellular TGFβ signalling components.

		average	count	p-value
ptc-Gal4 > UAS-pinguid crossed to:				
w[1118]	*white*	0.421	45	-
UAS-lacZ	*UAS-lacZ*	0.441	17	-
activin-beta[BG01941]	*activin-beta*	0.434	40	0.016
cv-2[1]	*crossveinless 2*	0.492	17	0.000
cv-2[225-3]	*crossveinless 2*	0.443	10	0.002
cv-2[3511]	*crossveinless 2*	0.424	7	0.788
dpp[d6]	*decapentaplegic*	0.451	5	0.002
dpp[hr4]	*decapentaplegic*	0.413	3	0.187
dpp[hr56]	*decapentaplegic*	0.473	6	0.000
dpp[s1]	*decapentaplegic*	0.449	18	0.000
gbb[1]	*glass bottom boat*	0.442	3	0.117
gbb[4]	*glass bottom boat*	0.450	3	0.009
scw[5]	*screw*	0.413	4	0.422
scw[l1]	*screw*	0.440	4	0.041
sog[S6]	*short gastrulation*	0.410	4	0.300
UAS-sog	*short gastrulation*	0.472	13	0.000

Figure 9 – Extracellular TGFβ signalling components. Examples of *ptc-Gal4, UAS-pinguid* crossed to (A) w^{1118}, (B) *UAS-lacZ*, (C) *activin-*$\beta^{BG01941}$, (D) *cv-*2^{1}, (E) *cv-*$2^{225\text{-}3}$, (F) *cv-*2^{3511}, (G) dpp^{d6}, (H) dpp^{hr4}, (I) dpp^{hr56}, (J) dpp^{s1}, (K) gbb^{1}, (L) gbb^{4}, (M) scw^{5}, (N) scw^{l1}, (O) sog^{S6}, and (P) *UAS-sog*.

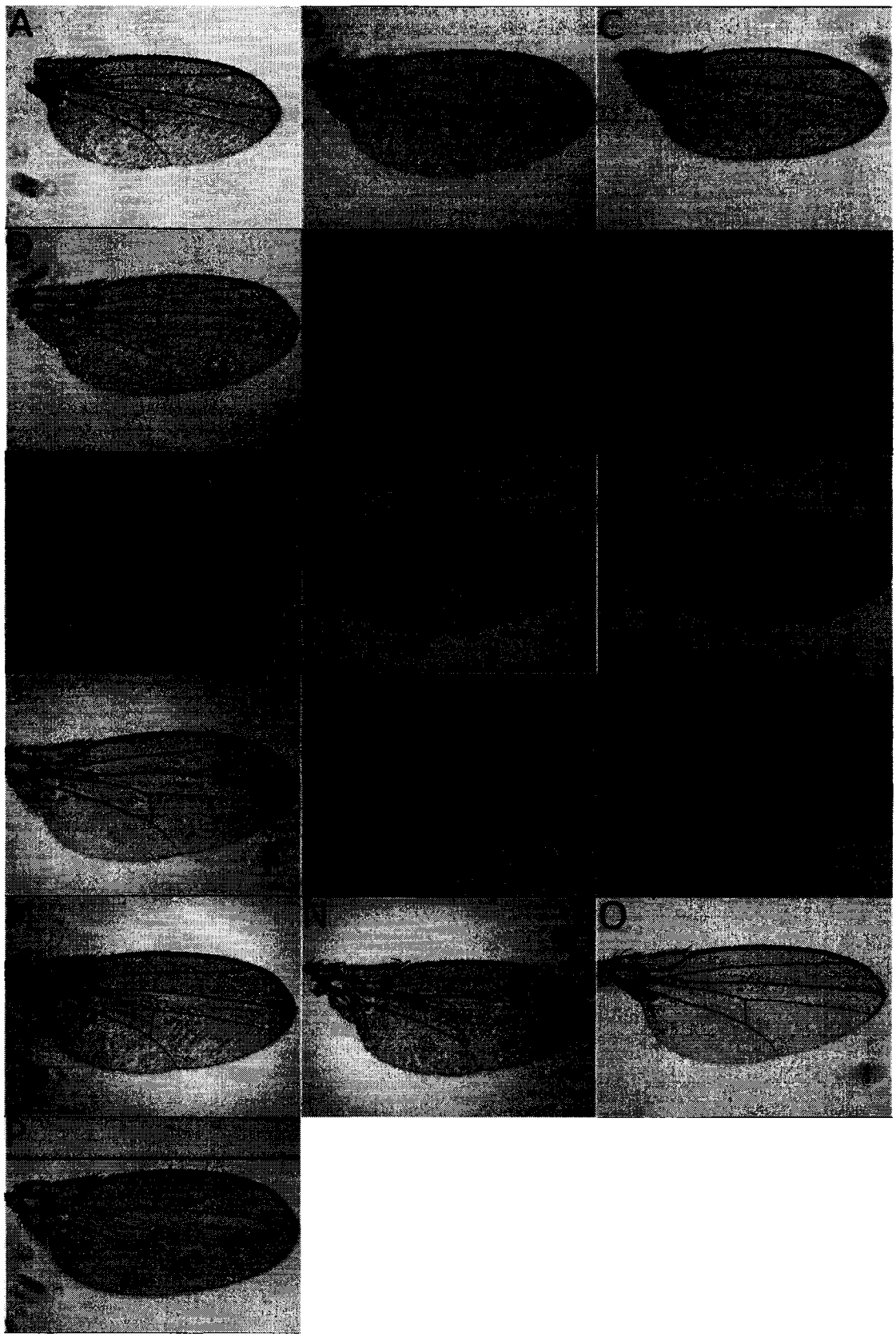
A
B
C
D
O

The analysis of *pinguid* continued next to the TGFβ receptors (Figure 10). No genetic interaction was seen with any of the type II receptor alleles tested. A mild, but statistically significant, enhancement was seen with two of the three *tkv* alleles tested (Table 5). One *babo* allele ($babo^{32}$) was visibly able to suppress the wing phenotype (Figure 10B, p = 0.000). Because the genetic interaction with *baboon* is so convincing and the signalling pathway through *baboon* is distinct from the *dpp* signalling pathway (Brummel et al., 1999), this suggests the *pinguid* may be acting through the Baboon-dSmad2 pathway instead of the Tkv-Mad pathway.

Table 5 – Receptors for TGFβ signalling.

		average	count	p-value
ptc-Gal4 > UAS-pinguid crossed to:				
w[1118]	*white*	0.421	45	-
babo[32]	*baboon*	0.499	18	0.000
babo[k16912]	*baboon*	0.437	4	0.262
put[135]	*punt*	0.430	3	0.479
sax[4]	*saxophone*	0.448	8	0.155
tkv[1]	*thickveins*	0.428	16	0.246
tkv[7]	*thickveins*	0.382	3	0.011
tkv[Sz-1]	*thickveins*	0.389	4	0.000
wit[A12]	*wishful thinking*	0.456	4	0.089
wit[B11]	*wishful thinking*	0.454	4	0.122

Figure 10 – Receptors for TGFβ signalling. Examples of *ptc-Gal4, UAS-pinguid* crossed to (A) w^{1118}, (B) $babo^{32}$, (C) $babo^{k16912}$, (E) put^{135}, (E) sax^{4}, (F) tkv^{1}, (G) tkv^{7}, (H) $tkv^{Sz\text{-}1}$, (I) wit^{A12}, and (J) wit^{B11}.

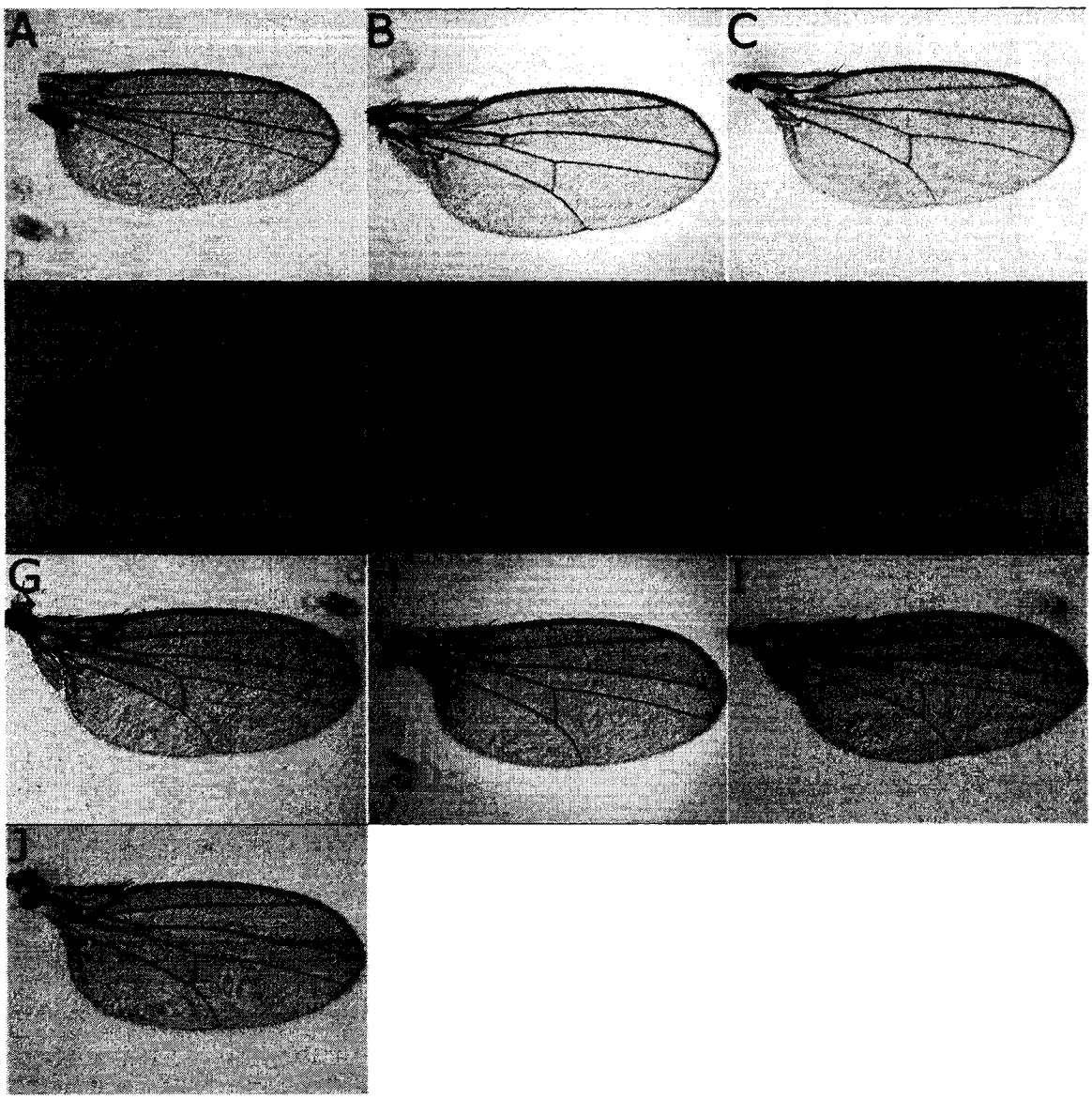
A
B
C
G
J

Next, the intracellular components of TGFβ were tested (Figure 11). Baboon binds and phosphorylates dSmad2 but not Mad (Brummel et al., 1999). No genetic interaction was seen with a dSmad2 allele ($Smox^{G0348}$, p = 0.902) but genetic interactions were seen with *Mad* and *Med* alleles. Three of the five *Mad* alleles tested statistically suppressed the wing phenotype (Table 6). Of the four *Med* alleles tested one enhanced the wing phenotype, two suppressed the phenotype, and the other allele had no affect. What these results mean for the role of *pinguid* in TGFβ signalling is unclear. While statistically significant, the suppression was not as visually convincing as the suppression with *babo*, and not all of the mutants showed an interaction. Tests with another allele of *dSmad2* (from Dr. Michael B. O'Connor, University of Minnesota), are planned to further characterize these interactions.

Table 6 – Intracellular TGFβ signalling components.

		average	count	p-value
ptc-Gal4 > UAS-pinguid crossed to:				
w[1118]	*white*	0.421	45	-
EcR[225]	*Ecdysone receptor*	0.480	18	0.000
EcR[k06210]	*Ecdysone receptor*	0.445	17	0.000
Med[13]	*Medea*	0.396	4	0.033
Med[2]	*Medea*	0.457	9	0.000
Med[3]	*Medea*	0.415	6	0.219
Med[4]	*Medea*	0.445	7	0.035
Mad[1-2]	*Mothers against dpp*	0.446	4	0.002
Mad[2]	*Mothers against dpp*	0.432	4	0.048
Mad[3]	*Mothers against dpp*	0.453	11	0.000
Mad[4]	*Mothers against dpp*	0.428	9	0.269
Mad[8-2]	*Mothers against dpp*	0.430	4	0.518
Smox[G0348]	*Smad on X (dSmad2)*	0.420	9	0.902

Figure 11 – Intracellular TGFβ signalling components. Examples of *ptc-Gal4, UAS-pinguid* crossed to (A) w^{1118}, (B) EcR^{225}, (C) EcR^{k06210}, (E) Med^{13}, (E) Med^{2}, (F) Med^{3}, (G) Med^{4}, (H) Mad^{1-2}, (I) Mad^{2}, (J) Mad^{3}, (K) Mad^{4}, (L) Mad^{8-2}, and (M) $Smox^{G0348}$.

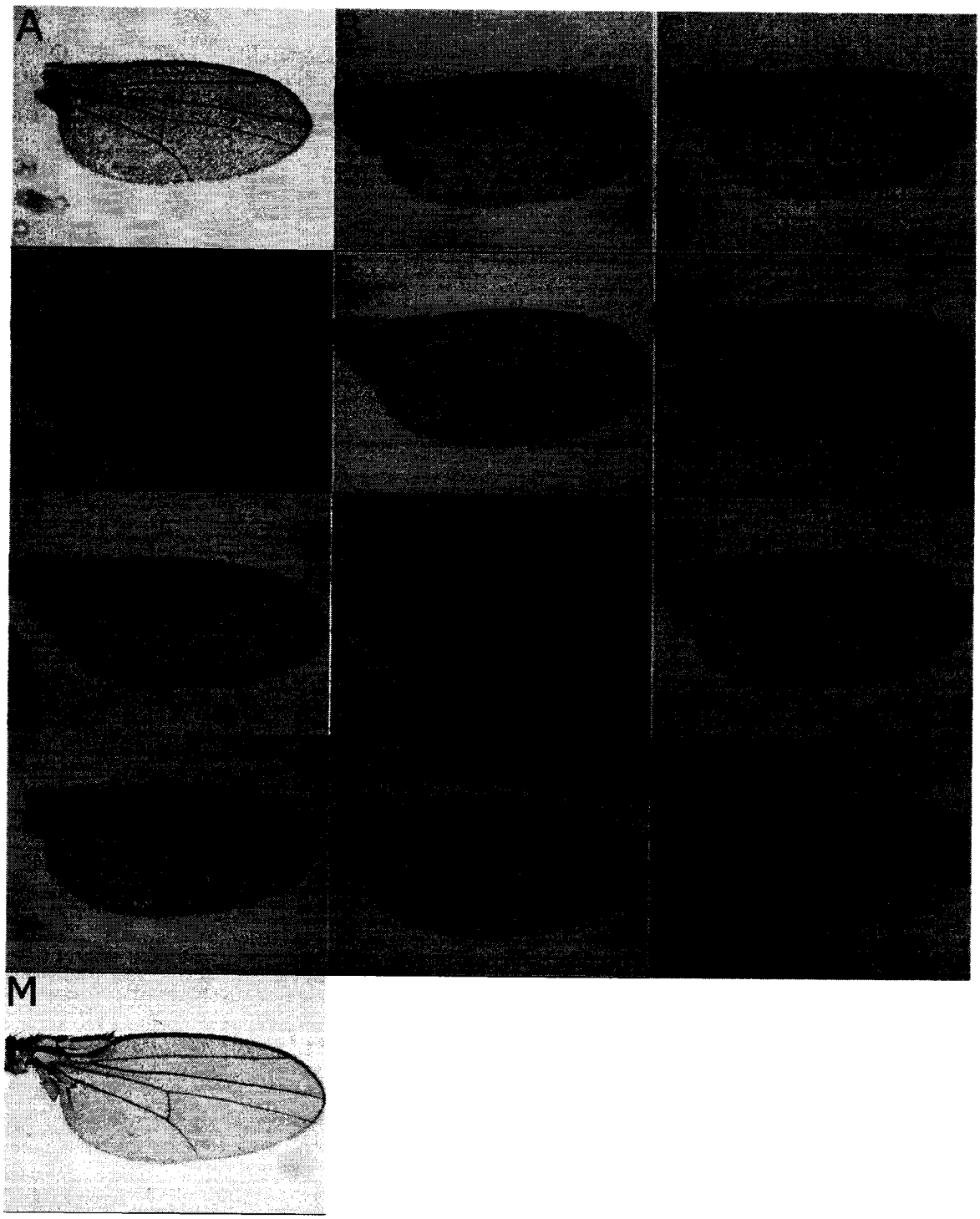
A
M

Activin signalling through Baboon and dSmad2 leads to transcription of the *Ecdysone receptor* gene (Zheng et al., 2003). One *EcR* allele (EcR^{225}) was able to significantly suppress the wing phenotype (Figure 11B, p = 0.000) while another allele (EcR^{k06210}) less visibly, but statistically, suppressed the wing phenotype (Figure 11C, p = 0.000). This result also suggests that Pinguid may be acting through the Baboon-dSmad2 pathway instead of the Tkv-Mad pathway.

DISCUSSION

The Drosophila homolog of Huntingtin interacting protein 14, *pinguid*, encodes an essential gene involved in TGFβ signalling. Expression of *pinguid* with *patched-Gal4* driver results in a mild phenotype: the L3-L4 intervein region is reduced by approximately 20% and the ACV is missing (Figure 7E). This wing phenotype is strongly suppressed by *cv-2*, *UAS-sog*, *babo*, and *EcR*. Genetic interactions were also seen with *dpp*, *tkv*, *Mad*, and *Med* alleles. But what role does *pinguid* play in TGFβ signalling?

One possible scenario is that Pinguid, a protein with sequence similarity to Hip14 and Akr1p, acts as a palmitoyltransferase. If the predicted DHHC domain is facing the cytoplasmic side of the Golgi (like Hip14 and Akr1p) than Pinguid may palmitoylate proteins with a cytoplasmic domain. What are potential substrates for palmitoylation in TGFβ signalling? Yck2p (Feng and Davis, 2000; Roth et al., 2002) and Ras (Rocks et al., 2005) are transiently associated with the plasma membrane and for both this association is palmitoylation dependent. In human tissue culture experiments SARA specifically recruits Smad2 to the plasma membrane to be phosphorylated by the type I receptor (Tsukazaki et al., 1998; Wu et al., 2000). In contrast, the Drosophila homolog plays a role in regulating Dpp signalling, although a potential role in Activin signalling has not been described (Bennett and Alphey, 2002). Could SARA's association with the plasma membrane be mediated by Pinguid-mediated palmitoylation? It

seems possible that, if SARA is palmitoylated and palmitoylation of SARA was Pinguid-mediated, over-expression of Pinguid could affect both the Activin and Dpp signalling pathways (as suggested by the results).

The human huntingtin protein is palmitoylated by Hip14 at an internal cysteine residue (C214) in a region conserved in the Drosophila homolog (Yanai et al., unpublished results). Assuming palmitoylation occurs at conserved residues, SARA was screened for potential cytosolic cysteines. SARA has 13 conserved cysteine residues over 1343 amino acids. Nine of these cysteines are within the predicted FYVE domain. The FYVE domain binds phosphatidylinositol 3-phosphate and mediates protein interactions with membranes (Tsukazaki et al., 1998). One cysteine is located within the Smad2 binding domain of SARA and the remaining three are located in the relatively well-conserved carboxyl-terminus of SARA. As there no common palmitoylation consensus site it is difficult to predict whether Pinguid could palmitoylate SARA. Palmitoylation of SARA by Pinguid would have to be tested biochemically as described by Huang et al., 2004.

Another possible scenario is that, when over-expressed, Pinguid binds to Sog and inhibits Sog function. In the developing wing, Dpp is negatively regulated by Sog, an extracellular protein that prevents Dpp diffusion (Eldar et al., 2002). A yeast two hybrid screen has identified Sog as a possible interactor of Pinguid (Giot et al., 2003). When Pinguid is over-expressed (presumably far above endogenous levels), Pinguid may bind and prevent Sog post-translational modifications, maturation, and/or secretion (Yu et al., 2000). Secretion of improperly processed Sog or less Sog could lead to the

mild defects seen in the *ptc-Gal4>UAS-pinguid* wing. A problem with this scenario is that Sog has no known role in Activin signalling.

pinguid encodes an essential protein although the timing of the lethal phase in homozygous mutants varies. Homozygous third instar larvae of the most severe excision alleles are rare while, in the least severe allele, homozygotes survive to the pharate adult stage. No visible defects have been observed so far. The morphology and patterning of the embryos appears normal, the development of the CNS looks wildtype, and the pharate adults have no visible external defects. Ideally, the role of *pinguid* in TGFβ signalling would be studied using these mutants. If *pinguid* plays a biologically relevant role in TGFβ signalling the expression of *salm*, *omb*, *vg*, of *EcR* should be affected. If a loss of function phenotype could be detected then the modulation TGFβ signalling could either enhance or suppress this phenotype. If not, the genetic interactions with TGFβ signalling components may just be an artefact of Pinguid over-expression.

MATERIALS AND METHODS

Protein alignment and domain prediction

Proteins were aligned using MacVector 6.5. The protein domains were identified using Pfam (Bateman et al., 2004; http://pfam.wustl.edu/) and the transmembrane domains were identified using TMHMM Server v. 2.0 (Moller et al., 2001; http://www.cbs.dtu.dk/services/TMHMM/).

Drosophila handling

Fly cultures and crosses were performed according to standard procedures. All crosses occurred at room temperature unless otherwise noted. In all cases, w^{1118} was used as a wildtype control. Left wings were dissected from adult female flies, washed in EtOH, and mounted in Aquatex (EM Science).

Drosophila stocks

The majority of the stocks were from the Bloomington Drosophila Stock Center at Indiana University (http://flystocks.bio.indiana.edu/). Other stocks were obtained from: Ethan Bier (University of California, San Diego); Seth S. Blair (University of Wisconsin, Madison); David L. Deitcher (Cornell University, Ithaca); Lawrence S. Goldstein (University of California, San Diego); Nicholas Harden (Simon Fraser University, Burnaby); Daniel Kalderon (Columbia University, New York); Laurel A. Raftery (Harvard Medical School,

Charlestown); and Kristi A. Wharton (Brown University, Providence). A number of transgenic stocks were created through the collaboration of Esther M. Verheyen (Simon Fraser University, Burnaby) and Michael R. Hayden (University of British Columbia, Vancouver).

Table 7 – Stocks

white	w[1118]	3605
lacZ	UAS-lacZ	NH
grim, reaper, head involution defective	Df(3L)H99, kni[ri-1] p[p]/TM3, Sb[1]	1576

Table 8 – Stocks: extracellular TGFβ signalling components

activin-beta	w[1118]; P{w[+mGT]=GT1}activin-beta[BG01941]/ey[D]	12648
crossveinless 2	cv-2[1]	6302
crossveinless 2	cv-2[225-3]	6342
crossveinless 2	cv-2[3511]	SSB
decapentaplegic	dpp[d6]/CyO	2062
decapentaplegic	dpp[hr4]/CyO	LAR
decapentaplegic	dpp[hr56]/CyO	LAR
decapentaplegic	dpp[s1]	397
glass bottom boat	gbb[1]/CyO	KAW
glass bottom boat	gbb[4]/CyO	KAW
screw	w[1118]; b[1] scw[5] pr[1]/CyO, P{ry[+t7.2]=sevRas1.V12}FK1	7306
screw	scw[l1] rdo[1] hk[1] pr[1]/CyO	4351
short gastrulation	y[1] sog[S6]/FM7c, sn[+]	2497
short gastrulation	UAS-sog/CyO	EB

Table 9 – Stocks: receptors for TGFβ signalling

baboon	w[*]; babo[32]/CyO	5399
baboon	y[1] w[67c23]; P{w[+mC]=lacW}babo[k16912]/CyO	11207
punt	st[1] put[135] e[1]/TM3, Ser[1]	3100
saxophone	y[1] w[*]; P{w[+mW.hs]=FRT(w[hs])}G13 sax[4]/SM6a	5404
thickveins	tkv[1]	427
thickveins	tkv[7] cn[1] bw[1] sp[1]/CyO	3242
thickveins	In(2L)tkv[Sz-1], al[1] tkv[Sz-1] b[1]/SM1	860
wishful thinking	bw[1]; wit[A12] st[1]/TM6B, Tb[1]	5173
wishful thinking	bw[1]; wit[B11] st[1]/TM6B, Tb[1]	5174

Table 10 – Stocks: intracellular TGFβ signalling components

Ecdysone receptor	w[1118]; EcR[225]/CyO	4899
Ecdysone receptor	y[1] w[67c23]; P{w[+mC]=lacW}EcR[k06210]/CyO	10614
Medea	ru[1] h[1] P{ry[+t7.2]=neoFRT}82B sr[1] e[s] Med[13]/TM3, Sb[1]	7340
Medea	Med[2]/TM6B	LAR
Medea	Med[3]/TM3	LAR
Medea	Med[4]/TM6B	LAR
Mothers against dpp	w[*]; Mad[1-2] P{ry[+t7.2]=neoFRT}40A/CyO	7323
Mothers against dpp	Mad[2]/SM6a	LAR
Mothers against dpp	Mad[3]/SM6a	LAR
Mothers against dpp	Mad[4]/SM6a	LAR
Mothers against dpp	w[*]; Mad[8-2] P{ry[+t7.2]=neoFRT}40A/CyO	7324
Smad on X	w[67c23] P{w[+mC]=lacW}Smox[G0348]/FM7c	12246

Wing measurements and statistical analysis

To quantitate wing pattern defects the distance between longitudinal vein three (L3) and L4 at the posterior crossvein (PCV) were measured as a fraction of the distance between L3 and L5 at the PCV (Figure 8). The probability of the means being significantly different was calculated using Student's t-Test with a two-tail distribution and two sample unequal variance. For mutants the average was compared to the average L3-L4/L3-L5 at the PCV for *ptc-Gal4, UAS-pinguid* crossed to w^{1118} (average = 0.421, n = 45). For UAS constructs the average was compared to the average L3-L4/L3-L5 at the PCV for *ptc-Gal4, UAS-pinguid* crossed to *UAS-lacZ* (average = 0.441, n = 17).

EY09853 and EP3292 excisions

EY09853/TM3 virgin females were crossed to *Δ2-3/TM6B* males. Male progeny containing both the *Δ2-3* transposase and the P-element were crossed to *TM3/TM6B* females. Single males that had lost one or both of the

two markers (*yellow*$^+$ and *white*$^+$) within the 11 kb P-element were crossed back to *TM3/TM6B* females to create a stock.

EP3292/TM3 virgin females were crossed to *Δ2-3/TM6B* males. Male progeny containing the *Δ2-3* transposase and the P-element were crossed to *TM3/TM6B* females. Single males that had lost the *white*$^+$ marker from the 8 kb P-element were crossed back to *TM3/TM6B* females to create a stock.

For the homozygous viable excisions, genomic DNA was isolated from males and PCR products were amplified using 3528-F and 5169-R (1.6kb PCR product; see Figure 12 and Table 11). Most PCR products were wildtype (1.6 kb) or slightly larger, indicating the presence of residual P-element sequence in the genome. Failure of this PCR suggested: (1) a significant amount of P-element sequence remains rendering the region too large to PCR amplify, (2) the 3528-F annealing site is deleted, (3) the 5169-R annealing site is deleted, or (4) both primer annealing are sites deleted. If this initial PCR failed, the PCR was repeated using four primers: 3528-F, 4197-R (0.7 kb product) and 4936-F, 7846-R (2.9 kb product). The combination of these PCR methods was used to reject all viable excisions as possible *pinguid* mutants, since they all showed bands indicating the gene was still intact.

The homozygous lethal excisions were crossed to *Df(3L)brm11* (72A3--72D5) and *Df(3L)XG5* (71C2--72C1) to confirm that the lethality was localized to the region of interest. Lethal excisions that were viable over *Df(3L)brm11* were discarded. A large number fell into this category (13 from EP3292 and 31 from EY09853) and were most likely due to second site mutations. The remaining lethal excisions were crossed to nine EMS mutants

that have been mapped to the *Df(3L)brm11* genetic interval but have not yet been assigned specific genes.

Isolation of genomic DNA

DNA was isolated from male flies as described at the Berkeley Drosophila Genome Project website (http://www.fruitfly.org/) with some modifications.

Five to 30 flies were frozen overnight at –80 ºC in a 1.5 ml eppendorf tube. The flies were ground in 200 ul of Buffer A (100 mM Tris-HCl, pH 7.5; 100 mM EDTA, pH 8.0; 100 mM NaCl; 0.5 % SDS); this was followed by an additional 200 ul of Buffer A and further grinding until no visible body parts were present. Following a 30 min incubation at 65 ºC, 800 ul of LiCl/KOAc solution (1 part 5 M KOAc; 2.5 parts 6 M LiCl) was added. This was allowed to incubate for at least 10 min on ice. After centrifuging at room temperature for 15 min (13,000 rpm, Eppendorf 5415C), 1 ml of the supernatant was transferred to a new tube containing 600 ul of isopropanol. After mixing the contents, the tube was centrifuged at room temperature for another 15 min at 13,000 rpm. The supernatant was removed and the pellet was washed with 500 ul of 70 % EtOH. The tube was centrifuged at room temperature for 5 min at 13,000 rpm, the EtOH removed, and the pellet allowed to dry (5 to 10 min at room temperature). The pellet was then re-suspended (5 ul per adult fly) in 1X TE (1 mM Tris-HCl, pH 8.0; 0.1 mM EDTA, pH 8.0) and stored at –20 ºC.

PCR from genomic DNA

PCR primers were designed using (Oligo 4.0-s) from a 12233 bp fragment from the Drosophila genome corresponding to 3L:15948884..15961116. The numbers correspond to their location on the 12 kb genomic fragment (the 5'end of the primer) and F and R indicate forward and reverse, respectively. The locations of the primer annealing sites are shown in Figure 12; the names, sequence, and annealing temperatures of the primers are shown in Table 11.

Primers were ordered from Invitrogen and initially re-suspended in 1X TE to 0.1 nmoles/ul. The primers were further diluted to 10 pmole/ul (1 uM) with ddH_2O. The PCR was performed as suggested in the manual for Taq DNA polymerase (Invitrogen, Life Technologies) but the total volume of the PCR reaction was scaled down to 20 ul.

Table 11 - Sequences of the PCR primers used for characterizing P-element excisions.

Name	Sequence	Tm
665-F	GCA AAA AAT CCA CGA ACC GAA AGA	67
3528-F	TTC CAC CAT AAG CAC AGC CTC CTG	69
4032-F	TAC TCA CCT GGG CTT CTT GGC ATG	69
Yellow-F	GGT GGC ATC ATC AGC ATC AAG GTT	68
White-R	TTA GAG CCA GAT ATG CGA GCA CCC	68
4197-R	GCT GCG GTC ACT CTA ACG TGC CTA	69
4465-F	TGG GGA TTG AAA ACC AGC GAG TAA	68
4936-F	ACC TCA GCG CAG TGT GAA TCA CGT	69
5169-R	CAC CAT ACT GGG TGG CCT TAA CGA	68
5911-R	GGC CTT TGA CTT GAG CAC GAG TGT	68
6422-R	CTC TGG TTG GTC GAA TGA TAC CGG	68
6936-R	CAA CAG GAT GAC CCA GGA CAT GTG	68
7295-R	GTT GGT TGT TAA ACA TGC GCG ATG	67
7846-R	CCA CAC ACC TCC GTG CAA ATC TCT	69
11191-R	AAC CAC ATT GTC TGC TCC GAC CAT	68

Figure 12 – Location of PCR primers used for characterizing P-element excisions. Sites of primer annealing are indicated by the arrowheads.

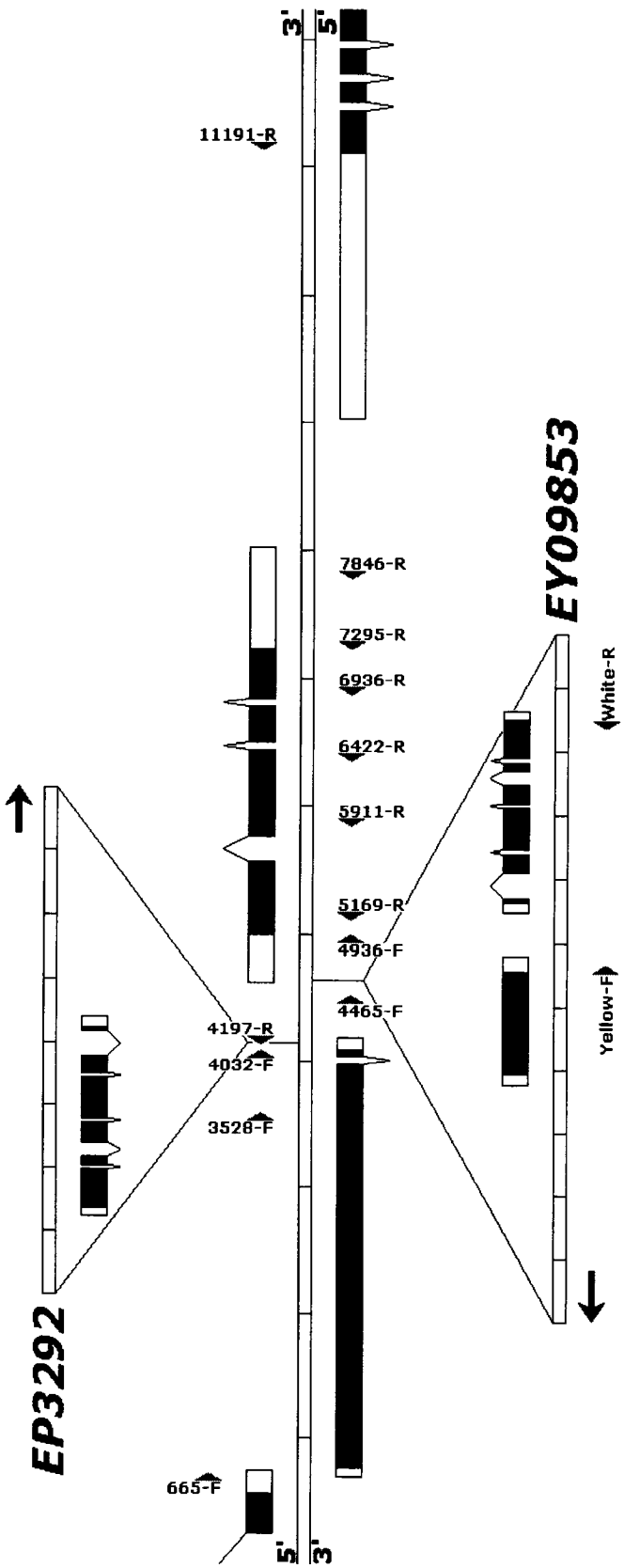
3'
5'
11191-R
7846-R
7295-R
6936-R
6422-R
5911-R
5169-R
4936-F
4465-F
4197-R
4032-F
3528-F
665-F
5'
3'
EP3292
EY09853
White-R
Yellow-F

Sequencing of the pinguid mutants

pinguid mutant virgin females were crossed to *EP3292* males. Genomic DNA was isolated from male *pinguid/EP3292* progeny. The *pinguid* strand was amplified by PCR using the 3528-F primer alone for 10 cycles. The entire region was then amplified using 3528-F and 7846-R; because EP3292 blocked PCR on one chromosome I was able to selectively amplify the *pinguid* mutant chromosome. The PCR fragments were separated on a 1% agarose gel (ethidium bromide). The bands were then excised and gel purified using the QIAquick Gel Extraction Kit (Qiagen) and stored in H_2O at −20 °C. The DNA was send to UBC for sequencing.

P{UAST} constructs

cDNAs were ordered from the Canadian Drosophila Microarray Centre, subcloned into pP{UAST} in the Hayden lab at the Centre for Molecular Medicine and Therapeutics (University of British Columbia), and injected by Justina Sanny at Simon Fraser University.

A 2.3 kb EcoRI fragment from LD10758 (Drosophila Hip14 homolog, CG6017) was cloned into pP{UAST}. This was constructed by David Klein and Martina Metzler at the CMMT and the DNA was sent to SFU as a 320 ng/ul Qiagen MIDIprep. Two transgenic strains were obtained: one each on the second and third chromosomes.

Preparation of pP{UAST} DNA for injection

DNA to be injected into embryos was prepared in the following manner: 40 ug of pP{UAST} was mixed with 8 ug of pTurbo and 1/10

volume of NaOAc, pH 5.2. After the addition of two volumes of cold 95 % EtOH, the DNA was mixed, and then allowed to precipitate for 30 min at -20 °C. The DNA was then centrifuged at room temperature for 30 min (13,000 rpm, Eppendorf 5415C) and the supernatant was discarded. This was followed by a wash with cold 70 % EtOH, centrifuging, discarding the supernatant, and allowing the DNA pellet to air dry at room temperature for 5 min. The DNA was then re-suspended in 80 ul of Injection Buffer (0.5 mM sodium phosphate, pH 7.5; 5 mM KCl).

Injecting embryos

w^{1118} embryos were collected on apple juice agar plates for 30 to 60 min. The embryos were dechorionated, aligned on a coverslip, briefly desiccated, and covered with halocarbon oil before injection. Hatching larvae were transferred to a fly food vial and allowed to develop. The surviving adults were crossed to w^{1118} and their progeny were screened for non-white eyes. Adults containing *white*$^{+}$ from the transgene were crossed back to w^{1118} to establish a stock.

Embryo collection and fixation for antibody staining

Embryos were collected on apple juice agar plates (supplemented with yeast paste) for 16 hrs at 25 °C. Excess yeast and dead flies were removed from the plate before the addition of water. A paintbrush was used to loosen the embryos from the agar and to transfer the embryos into a mesh basket where they were rinsed with water. Once rinsed the embryos were dechorionated in 50 % bleach (diluted with water) for 3 to 5 min. The basket

was removed from the bleach, dried briefly on a paper towel, and then washed twice in water for at least 30 sec each. The embryos were then transferred into a scintillation vial containing Fixation Buffer (4 ml 1X PBS; 5 ml heptane; 1 ml 20 % paraformaldehyde) and fixed (with shaking) for 25 min. The heptane and aqueous layers were allowed time to separate and the lower aqueous phase was removed and replaced with 5 ml of MeOH. The vial was then shaken vigorously for 1 min to aid in removal of the vitelline membrane; the devitellinized embryos sink to the bottom of the vial. Most of the liquid was removed and replaced with MeOH. The embryos were rinsed twice more with MeOH, transferred to a 1.5 ml eppendorf tube and stored at -20 ºC.

Antibody staining using an HRP secondary

Fixed embryos in MeOH were re-hydrated by washing 3 times with PBST (1X PBS; 0.1 % Triton X-100) for 10 min each. Embryos were then blocked by incubating with PBT (1X PBS; 0.1 % Triton X-100; 2 mg/ml BSA) for 60 min on a rotator. The PBT was removed and replaced by the primary antibody diluted in PBT. The primary antibody was incubated with the embryos overnight at 4 ºC on a rotator.

The next day the PBT containing the antibody was removed and saved and the embryos were washed three times with PBST for 10 min each. The PBST was removed and replaced by the secondary antibody diluted (1:200) in PBT. This was allowed to incubate for 2 to 3 hrs at room temperature on a rocker. Following this incubation the PBT containing the antibody was

removed and the embryos were washed three times with PBST for 10 min each.

For the black horseradish peroxidase reaction the embryos were incubated in DAB-Ni Solution (500 ul 8 % $NiCl_2$; 500 ul 1X PBS; 50 ul of DAB (5mg/ml 3,3'-diaminobenzidine)) for 2 min to allow penetration into the embryos. The reaction was initiated by adding 1 ul of 3 % H_2O_2 and monitored with a dissecting microscope until the reaction had progressed to the desired point. Excess DAB-Ni Solution was removed and the embryos were washed three times with PBST for 10 min each. After allowing the embryos to equilibrate in 50 % glycerol, they were transferred to a slide and viewed under a light microscope.

Antibodies used

The following antibodies were obtained from the Developmental Studies Hybridoma Bank at the University of Iowa: mouse-α-slit, mouse-α-DGluR-IIA, rat-α-elav (1:100), mouse-α-BPP102 (1:200), mouse-α-robo, mouse-α-wit, and mouse-α-dlg1 (1:100). Rabbit-α-synaptotagmin (1:500) was obtained from Hugo Bellen (Baylor College of Medicine). Rabbit-α-Pak (1:1000) was obtained from Nicholas Harden (Simon Fraser University). Other antibodies used included mouse-α-GFP (1:2000), HRP-conjugated goat-α-mouse (1:200), HRP-conjugated goat-α-rabbit (1:200), and HRP-conjugated goat-α-rat (1:200).

Recombination of Gal4 drivers onto a *UAS-pinguid* chromosome

UAS-pinguid virgin females were crossed to *X-Gal4* males, where X represents a number of Gal4 insertions. Female progeny containing the UAS-pinguid/X-Gal4 were crossed to *TM3/TM6B* or *Sp/CyO* males, depending on whether the *pinguid* transgene and Gal4 were on the second or third chromosome respectively. The male progeny that expressed the expected *X-Gal4>UAS-pinguid* wing phenotype were crossed back to *TM3/TM6B* or *Sp/CyO* females to establish a stock. I was only able to establish and maintain recombinant lines with *30A-Gal4* (four lines) and *ptc-Gal4* (five lines). Only the *ptc-Gal4, UAS-pinguid* recombinants were used for further studies.

APPENDIX

Table 12 – Potential Hip14 substrates

		average	count	p-value
ptc-Gal4 > UAS-pinguid crossed to:				
w[1118]	*white*	0.421	45	-
dlg1[G0276]	*discs large 1*	0.410	4	0.040
dlg1[G0342]	*discs large 1*	0.399	4	0.004
dlg1[G0456]	*discs large 1*	0.415	4	0.267
Gad1[A8]	*Glutamic acid decarboxylase 1*	0.391	4	0.037
Gad1[B9]	*Glutamic acid decarboxylase 1*	0.418	4	0.755
Gad1[L352F]	*Glutamic acid decarboxylase 1*	0.427	2	0.794
syt[N6]	*synaptotagmin*	0.459	6	0.003
syt[T77]	*synaptotagmin*	0.446	6	0.000

Table 13 – Stocks: potential Hip14 substrates

discs large 1	w[67c23] P{w[+mC]=lacW}dlg1[G0276]/FM7c	11876
discs large 1	w[67c23] P{w[+mC]=lacW}dlg1[G0342]a P{lacW}dlg1[G0342]b dlg1[G0342]/FM7c	11976
discs large 1	w[67c23] P{w[+mC]=lacW}dlg1[G0456]/FM7c	12301
Glutamic acid decarboxylase 1	bw[1]; Gad1[A8] st[1]/TM6B, Tb[+]	5186
Glutamic acid decarboxylase 1	bw[1]; Gad1[B9] st[1]/TM6B, Tb[+]	5187
Glutamic acid decarboxylase 1	Gad1[L352F], e[s]/TM3, Sb[1] Ser[1]	6295
synaptotagmin	y[1] w[*]; Df(2L)N6, P{w[+mC]=lacW}B8-2-30, syt[N6]/CyO	3910
synaptotagmin	y[1] w[*]; P{w[+mC]=lacW}syt[T77]/CyO	4377

Table 14 - Huntingtin

		average	count	p-value
ptc-Gal4 > UAS-pinguid crossed to:				
w[1118]	*white*	0.421	45	-
UAS-lacZ	*UAS-lacZ*	0.441	17	-
Df(3R)Exel6210	*huntingtin*	0.417	5	0.685
UAS-128QC-Ia	*huntingtin*	0.420	3	0.258
UAS-128QS-IId	*huntingtin*	0.440	4	0.906
UAS-128QS-IIId	*huntingtin*	0.416	4	0.056
UAS-httRNAi-I	*huntingtin*	0.422	4	0.217
UAS-httRNAi-III	*huntingtin*	0.418	4	0.015

Table 15 – Stocks: huntingtin

huntingtin	w[1118]; Df(3R)Exel6210, P{w[+mC]=XP-U}Exel6210/TM6B, Tb[1]	7688
huntingtin	w[1118] UAS-htt128QC-Xa	EMV
huntingtin	y[1] w[1118]; UAS-htt128QS-IId/CyO	EMV
huntingtin	y[1] w[1118]; UAS-htt128QS-IIId/TM3, Sb[1]	EMV
huntingtin	UAS-httRNAi-I	LSG
huntingtin	UAS-httRNAi-III	LSG

Table 16 – Glutamate receptors

		average	count	p-value
ptc-Gal4 > UAS-pinguid crossed to:				
w[1118]	*white*	0.421	45	-
Df(2L)Exel7023	*GluRIIA & GluRIIB*	0.469	4	0.000
Df(2L)Exel8016	*GluRIIA & GluRIIB*	0.460	2	0.003
Glu-RI[f05411]	*Glutamate receptor I*	0.474	28	0.000
Glu-RIB[f01757]	*Glutamate receptor IB*	0.425	4	0.687

Table 17 – Stocks: glutamate receptors

GluRIIA & GluRIIB	w[1118]; Df(2L)Exel7023, P+PBac{XP5.WH5}Exel7023/CyO	7798
GluRIIA & GluRIIB	w[1118]; Df(2L)Exel8016, P+PBac{XP5.WH5}Exel8016/CyO	7797
Glutamate receptor I	w[1118]; PBac{w[+mC]=WH}Glu-RI[f05411]	18860
Glutamate receptor IB	w[1118]; PBac{w[+mC]=WH}Glu-RIB[f01757]/TM6B, Tb[1]	18468

Table 18 – Alsin and Hip1

		average	count	p-value
ptc-Gal4 > UAS-pinguid crossed to:				
w[1118]	*white*	0.421	45	-
UAS-lacZ	*UAS-lacZ*	0.441	17	-
CG7158[f01748]	*Alsin*	0.433	9	0.117
UAS-Alsin-I	*Alsin*	0.432	10	0.397
UAS-Alsin-II	*Alsin*	0.420	8	0.011
UAS-Alsin-III	*Alsin*	0.437	10	0.673
Df(3L)Exel6117	*Hip1*	0.434	4	0.146
UAS-Hip1-IIc	*Hip1*	0.418	4	0.135
UAS-Hip1-IIIb	*Hip1*	0.433	4	0.756

Table 19 – Stocks: Alsin and Hip1

Alsin	w[1118]; PBac{w[+mC]=WH}CG7158[f01748]	18467
Alsin	w[1118] UAS-CG7158-I	EMV
Alsin	y[1] w[1118]; UAS-CG7158-II/CyO	EMV
Alsin	y[1] w[1118]; UAS-CG7158-III/TM3, Sb[1]	EMV
Hip1	w[1118]; Df(3L)Exel6117, P{w[+mC]=XP-U}Exel6117/TM6B, Tb[1]	7596
Hip1	y[1] w[1118]; UAS-CG10971-IIc/CyO	EMV
Hip1	y[1] w[1118]; UAS-CG10971-IIIa/TM3, Sb[1]	EMV

Table 20 – Endocytosis, exocytosis, and intracellular protein transport

		average	count	p-value
ptc-Gal4 > UAS-pinguid crossed to:				
w[1118]	*white*	0.421	45	-
alpha-Adaptin[06694]	*alpha-Adaptin*	0.400	4	0.031
Amph[26]	*Amphiphysin*	0.449	4	0.242
CG10882[KG02906]	*CG10882*	0.457	7	0.000
Chc[1]	*Clathrin heavy chain*	0.394	1	N/A
Chc[4]	*Clathrin heavy chain*	0.454	4	0.058
dor[8]	*deep orange*	0.417	12	0.517
garz[EP2028]	*gartenzwerg*	0.421	4	0.957
gig[109]	*gigas*	0.428	8	0.523
hk[1]	*hook*	0.411	4	0.025
l(2)06496[06496]	*lethal (2) 06496*	0.400	5	0.043
Lis-1[k11702]	*Lissencephaly-1*	0.383	6	0.016
milt[k04704]	*milton*	0.395	6	0.029
Rab5[k08232]	*Rab-protein 5*	0.427	7	0.357
shi[1]	*shibire*	0.431	4	0.482
Snap25[695]	*Synapse protein 25*	0.404	9	0.005
Syb[k07703]	*Synaptobrevin*	0.433	4	0.103
Syx1A[06737]	*Syntaxin 1A*	0.443	4	0.009
Syx1A[Delta229]	*Syntaxin 1A*	0.374	4	0.001
Tapdelta[k17005]	*Translocon-associated protein δ*	0.419	5	0.788

Table 21 – Stocks: endocytosis, exocytosis, and intracellular protein transport

alpha-Adaptin	cn[1] P{ry[+t7.2]=PZ}alpha-Adaptin[06694]/CyO; ry[506]	12319
Amphiphysin	w[*]; Amph[26]	6498
CG10882	y[1]; P{y[+mDint2] w[BR.E.BR]=SUPor-P}CG10882[KG02906]/CyO; ry[506]	13336
Clathrin heavy chain	w[*] Chc[1]/FM7c/Dp(1;Y)shi[+]1, y[+] B[S]	4166
Clathrin heavy chain	w[*] Chc[4]/FM7c	4167
deep orange	dor[8]/FM6	28
gartenzwerg	w[1118]; P{w[+mC]=EP}garz[EP2028]/CyO	17017
gigas	mwh[1] jv[1] gig[109] red[1] ro[1]/TM3, Ser[1]	4739
hook	hk[1]	306
lethal (2) 06496	P{ry[+t7.2]=PZ}l(2)06496[06496] cn[1]/CyO; ry[506]	12316
Lissencephaly-1	y[1] w[67c23]; P{w[+mC]=lacW}Lis-1[k11702]/CyO	10179
milton	y[1] w[67c23]; P{w[+mC]=lacW}milt[k04704]/CyO	10553
Rab-protein 5	y[1] w[67c23]; P{w[+mC]=lacW}Rab5[k08232]/CyO	10786
shibire	w[1118] shi[1]/FM6	7068
Synapse protein 25	Snap25[695]/TM3 Sb Ser	DD
Synaptobrevin	y[1] w[67c23]; P{w[+mC]=lacW}Syb[k07703]/CyO	10678
Syntaxin 1A	ry[506] P{ry[+t7.2]=PZ}Syx1A[06737]/TM3, ry[RK] Sb[1] Ser[1]	11697
Syntaxin 1A	Syx1A[Delta229] ry[506]/TM3, ry[RK] Sb[1] Ser[1]	4379
Translocon-associated protein δ	y[1] w[67c23]; P{w[+mC]=lacW}Tapdelta[k17005]/CyO	11222

Table 22 – Nervous system development

		average	count	p-value
ptc-Gal4 > UAS-pinguid crossed to:				
w[1118]	*white*	0.421	45	-
eys[BG02208]	*eyes shut*	0.423	7	0.756
inv[30]	*invected*	0.424	5	0.772
l(2)gl[01433]	*lethal (2) giant larvae*	0.438	4	0.049
neur[1]	*neuralized*	0.443	2	0.350
Df(3R)M-Kx1	*prospero*	0.418	7	0.727
pros[17]	*prospero*	0.430	9	0.155
spen[03350]	*split ends*	0.451	6	0.012
stan[192]	*starry night*	0.441	2	0.264

Table 23 – Stocks: nervous system development

eyes shut	w[1118]; P{w[+mGT]=GT1}eys[BG02208]	12661
invected	inv[30]/SM5	7088
lethal (2) giant larvae	l(2)gl[01433] P{ry[+t7.2]=PZ}kek1[01433] l(2)36Ba[01433] cn[1]/CyO; ry[506]	11053
neuralized	ru[1] h[1] th[1] st[1] neur[1] cu[1] sr[1] e[s] ca[1]/TM3, Sb[1]	4222
prospero	w[*]; pros[17]/TM6B, Tb[1]	5458
prospero	Df(3R)M-Kx1/TM3, Sb[1]	3128
split ends	P{ry[+t7.2]=PZ}spen[03350] cn[1]/CyO; ry[506]	11295
starry night	w[1118]; P{ry[+t7.2]=neoFRT}42D stan[192]/CyO	6969

Table 24 – Palmitoyltransferases

		average	count	p-value
ptc-Gal4 > UAS-pinguid crossed to:				
w[1118]	*white*	0.421	45	-
Df(3L)brm11	*pinguid*	0.445	5	0.156
l(3)72Ad[I25]	*pinguid*	0.443	5	0.052
l(3)72Ad[K8]	*pinguid*	0.444	5	0.059
ping[X1]	*pinguid*	0.456	5	0.016
ping[X2]	*pinguid*	0.442	7	0.030
ping[X3]	*pinguid*	0.420	6	0.915
por[15175]	*porcupine*	0.429	16	0.235
l(3)63Bg[1]	*rasp*	0.405	12	0.008

Table 25 – Stocks: palmitoyltransferases

pinguid	Df(3L)brm11/TM6C, cu[1] Sb[1] ca[1]	3640
pinguid	w[1118]; l(3)72Ad[I25] P{w[+m*]=*}71F/TM3, Sb[1]	4111
pinguid	w[1118]; l(3)72Ad[K8] P{w[+m*]=*}71F/TM3, Sb[1]	DK
pinguid	y[1] w[1118]; ping[X1]/TM3, Sb[1]	BA
pinguid	y[1] w[1118]; ping[X2]/TM3, Sb[1]	BA
pinguid	y[1] w[1118]; ping[X3]/TM3, Sb[1]	BA
porcupine	por[15175] os[s]/FM6, w[1]	4740
rasp	l(3)63Bg[1]/TM6B, Tb[1]	2438

Table 26 – Cell proliferation

		average	count	p-value
ptc-Gal4 > UAS-pinguid crossed to:				
w[1118]	*white*	0.421	45	-
ft[1]	*fat*	0.417	4	0.836
twi[1]	*twist*	0.411	7	0.210
wee[ES1]	*wee*	0.398	5	0.094

Table 27 – Stocks: cell proliferation

fat	ft[1]	304
twist	cn[1] twi[1] bw[1] sp[1]/CyO	2381
wee	w[1]; wee[ES1] cn[1]/CyO, P{w[+mC]=ActGFP}JMR1	5833

Table 28 – Other signalling pathways

genotype		average	count	p-value
w[1118]	*white*	0.421	45	-
bhe[1]	*broad head*	0.426	3	0.389
caps[02937]	*capricious*	0.420	4	0.867
Cdc42[1]	*cdc42*	0.382	7	0.002
Cdc42[2]	*cdc42*	0.412	12	0.122
Cdc42[3]	*cdc42*	0.429	5	0.231
Cdc42[4]	*cdc42*	0.390	9	0.000
cv[1]	*crossveinless*	0.458	2	0.000
cv-c[1]	*crossveinless c*	0.454	2	0.235
dos[P115]	*daughter of sevenless*	0.462	4	0.008
dsh[3]	*dishevelled*	0.411	4	0.201
l(2)k01206[k01206]	*lethal (2) k01206*	0.434	7	0.072
pnut[02502]	*peanut*	0.455	4	0.021
pnut[KG00478]	*peanut*	0.440	7	0.016
shn[1]	*schnurri*	0.397	6	0.004
skf[BG02148]	*skiff*	0.433	6	0.296
sty[226]	*sprouty*	0.412	3	0.556
shark[1]	*Src homology 2, ankyrin repeat, tyrosine kinase*	0.436	7	0.354
wg[l-17]	*wingless*	0.408	6	0.077
Wnt4[EMS23]	*Wnt oncogene analog 4*	0.407	3	0.455

Table 29 – Stocks: other signalling pathways

broad head	bhe[1] cn[1] bw[1] sp[1]/CyO	3268
capricious	P{ry[+t7.2]=PZ}caps[02937] ry[506]/TM3, ry[RK] Sb[1] Ser[1]	11579
cdc42	y[1] w[*] Cdc42[1]/FM6	NH
cdc42	y[1] w[*] Cdc42[2]	NH
cdc42	w[1] sn[3] Cdc42[3]/FM6	NH
cdc42	y[1] w[*] Cdc42[4]/FM6	NH
crossveinless	y[1] cv[1]	4182
crossveinless c	cv-c[1]	472
daughter of sevenless	w[*]; P{w[+mC]=lacW}dos[P115] th[1] cu[1] sr[1]/TM6B, Tb[1]	6845
dishevelled	w[*] dsh[3] P{ry[+t7.2]=neoFRT}19A/FM7a	6331
lethal (2) k01206	y[1] w[67c23]; P{w[+mC]=lacW}l(2)k01206[k01206]/CyO	10493
peanut	cn[1] P{ry[+t7.2]=PZ}pnut[02502]/CyO; ry[506]	11194
peanut	y[1]; P{y[+mDint2] w[BR.E.BR]=SUPor-P}pnut[KG00478]/SM6a	14354
schnurri	cn[1] shn[1] bw[1] sp[1]/CyO	3008
skiff	w[1118]; P{w[+mGT]=GT1}skf[BG02148]	12656
sprouty	w[*]; sty[226] h[1] ca[1]/TM6B, Tb[1]	6383
Src homology 2, ankyrin repeat, tyrosine kinase	P{ry[+t7.2]=neoFRT}43D shark[1]/CyO	5865
wingless	wg[l-17] b[1] pr[1]/CyO	2980
Wnt oncogene analog 4	Wnt4[EMS23] bw[1]/CyO, P{ry[+t7.2]=HB-lacZ}GS1	6650

REFERENCES

Bateman A, Coin L, Durbin R, Finn RD, Hollich V, Griffiths-Jones S, Khanna A, Marshall M, Moxon S, Sonnhammer EL, Studholme DJ, Yeats C, Eddy SR. (2004) The Pfam protein families database. Nucleic Acids Research 32, D138-D141.

Bates GP. (2005) History of genetic disease: the molecular genetics of Huntington disease - a history. Nature Reviews Genetics 6, 766-773.

Bellen HJ, Levis RW, Liao G, He Y, Carlson JW, Tsang G, Evans-Holm M, Hiesinger PR, Schulze KL, Rubin GM, Hoskins RA, Spradling AC. (2004) The BDGP gene disruption project: single transposon insertions associated with 40% of Drosophila genes. Genetics 167, 761-781.

Bennett D, Alphey L. (2002) PP1 binds Sara and negatively regulates Dpp signaling in Drosophila melanogaster. Nature Genetics 31, 419-423.

Brand AH, Perrimon N. (1993) Targeted gene expression as a means of altering cell fates and generating dominant phenotypes. Development 118, 401-415.

Brizuela BJ, Elfring L, Ballard J, Tamkun JW, Kennison JA. (1994) Genetic analysis of the brahma gene of Drosophila melanogaster and polytene chromosome subdivisions 72AB. Genetics 137, 803-813.

Brummel T, Abdollah S, Haerry TE, Shimell MJ, Merriam J, Raftery L, Wrana JL, O'Connor MB. (1999) The Drosophila activin receptor baboon signals through dSmad2 and controls cell proliferation but not patterning during larval development. Genes and Development 13, 98-111.

Camp LA, Hofmann SL. (1993) Purification and properties of a palmitoyl-protein thioesterase that cleaves palmitate from H-Ras. Journal of Biological Chemistry 268, 22566- 22574.

Capdevila J, Estrada MP, Sanchez-Herrero E, Guerrero I. (1994) The Drosophila segment polarity gene patched interacts with decapentaplegic in wing development. EMBO Journal 13, 71-82.

Chamoun Z, Mann RK, Nellen D, von Kessler DP, Bellotto M, Beachy PA, Basler K. (2001) Skinny hedgehog, an acyltransferase required for palmitoylation and activity of the hedgehog signal. Science 293, 2080-2084.

Chiang CS, Lehman IR. (1995) Isolation and sequence determination of the cDNA encoding DNA polymerase delta from Drosophila melanogaster. Gene 166, 237-242.

Conley CA, Silburn R, Singer MA, Ralston A, Rohwer-Nutter D, Olson DJ, Gelbart W, Blair SS. (2000) Crossveinless 2 contains cysteine-rich domains and is required for high levels of BMP-like activity during the formation of the cross veins in Drosophila. Development 127, 3947-3959.

el-Husseini Ael-D, Bredt DS. (2002) Protein palmitoylation: a regulator of neuronal development and function. Nature Reviews Neuroscience 3, 791-802.

Eldar A, Dorfman R, Weiss D, Ashe H, Shilo BZ, Barkai N. (2002) Robustness of the BMP morphogen gradient in Drosophila embryonic patterning. Nature 419, 304-308.

Featherstone DE, Rushton EM, Hilderbrand-Chae M, Phillips AM, Jackson FR, Broadie K. (2000) Presynaptic glutamic acid decarboxylase is required for induction of the postsynaptic receptor field at a glutamatergic synapse. Neuron 27, 71-84.

Feng Y, Davis NG. (2000) Akr1p and the type I casein kinases act prior to the ubiquitination step of yeast endocytosis: Akr1p is required for kinase localization to the plasma membrane. Molecular and Cellular Biology 20, 5350-5359.

Giot L, Bader JS, Brouwer C, Chaudhuri A, Kuang B, Li Y, Hao YL, Ooi CE, Godwin B, Vitols E, Vijayadamodar G, Pochart P, Machineni H, Welsh M, Kong Y, Zerhusen B, Malcolm R, Varrone Z, Collis A, Minto M, Burgess S, McDaniel L, Stimpson E, Spriggs F, Williams J, Neurath K, Ioime N, Agee M, Voss E, Furtak K, Renzulli R, Aanensen N, Carrolla S, Bickelhaupt E, Lazovatsky Y, DaSilva A, Zhong J, Stanyon CA, Finley RL Jr, White KP, Braverman M, Jarvie T, Gold S, Leach M, Knight J, Shimkets RA, McKenna MP, Chant J, Rothberg JM. (2003) A protein interaction map of Drosophila melanogaster. Science 302, 1727-1736.

Givan SA, Sprague GF Jr. (1997) The ankyrin repeat-containing protein Akr1p is required for the endocytosis of yeast pheromone receptors. Molecular Biology of the Cell 8, 1317-1327.

Goodwin JS, Drake KR, Rogers C, Wright L, Lippincott-Schwartz J, Philips MR, Kenworthy AK. (2005) Depalmitoylated Ras traffics to and from the Golgi complex via a nonvesicular pathway. Journal of Cell Biology 170, 261-272.

Gunawardena S, Her LS, Brusch RG, Laymon RA, Niesman IR, Gordesky-Gold B, Sintasath L, Bonini NM, Goldstein LS. (2003) Disruption of axonal transport by loss of huntingtin or expression of pathogenic polyQ proteins in Drosophila. Neuron 40, 25-40.

Hofmann K. (2000) A superfamily of membrane-bound O-acyltransferases with implications for wnt signaling. Trends in Biochemical Sciences 25, 111-112.

Huang K, Yanai A, Kang R, Arstikaitis P, Singaraja RR, Metzler M, Mullard A, Haigh B, Gauthier-Campbell C, Gutekunst CA, Hayden MR, El-Husseini A. (2004) Huntingtin-interacting protein HIP14 is a palmitoyl transferase involved in palmitoylation and trafficking of multiple neuronal proteins. Neuron 44, 977-986.

Huntington's Disease Collaborative Research Group. (1993) A novel gene containing a trinucleotide repeat that is expanded and unstable on Huntington's disease chromosomes. Cell 72, 971-983.

Kao LR, Peterson J, Ji R, Bender L, Bender A. (1996) Interactions between the ankyrin repeat-containing protein Akr1p and the pheromone response pathway in Saccharomyces cerevisiae. Molecular and Cellular Biology 16, 168-178.

Kraut R, Menon K, Zinn K. (2001) A gain-of-function screen for genes controlling motor axon guidance and synaptogenesis in Drosophila. Current Biology 11, 417-430.

Lahey T, Gorczyca M, Jia XX, Budnik V. (1994) The Drosophila tumor suppressor gene dlg is required for normal synaptic bouton structure. Neuron 13, 823-835.

Lecuit T, Cohen SM. (1998) Dpp receptor levels contribute to shaping the Dpp morphogen gradient in the Drosophila wing imaginal disc. Development 125, 4901-4907.

Lee JD, Treisman JE. (2001) Sightless has homology to transmembrane acyltransferases and is required to generate active Hedgehog protein. Current Biology 11, 1147-1152.

Li Z, Karlovich CA, Fish MP, Scott MP, Myers RM. (1999) A putative Drosophila homolog of the Huntington's disease gene. Human Molecular Genetics 8, 1807-1815.

Linder ME, Deschenes RJ. (2004) Model organisms lead the way to protein palmitoyltransferases. Journal of Cell Science 117, 521-526.

Linder ME, Deschenes RJ. (2003) New insights into the mechanisms of protein palmitoylation. Biochemistry 42, 4311-4320.

Littleton JT, Stern M, Schulze K, Perin M, Bellen HJ. (1993) Mutational analysis of Drosophila synaptotagmin demonstrates its essential role in Ca(2+)-activated neurotransmitter release. Cell 74, 1125-1134.

Lobo S, Greentree WK, Linder ME, Deschenes RJ. (2002) Identification of a Ras palmitoyltransferase in Saccharomyces cerevisiae. Journal of Biological Chemistry 277, 41268-41273.

Marquez RM, Singer MA, Takaesu NT, Waldrip WR, Kraytsberg Y, Newfeld SJ. (2001) Transgenic analysis of the Smad family of TGF-β signal transducers in Drosophila melanogaster suggests new roles and new interactions between family members. Genetics 157, 1639-1648.

Melendez A, Li W, Kalderon D. (1995) Activity, expression and function of a second Drosophila protein kinase A catalytic subunit gene. Genetics 141, 1507-1520.

Micchelli CA, The I, Selva E, Mogila V, Perrimon N. (2002) Rasp, a putative transmembrane acyltransferase, is required for Hedgehog signaling. Development 129, 843-851.

Morfini G, Pigino G, Brady ST. (2005) Polyglutamine expansion diseases: failing to deliver. Trends in Molecular Medicine 11, 64-70.

Moller S, Croning MD, Apweiler R. (2001) Evaluation of methods for the prediction of membrane spanning regions. Bioinformatics 17, 646-653.

Nellen D, Burke R, Struhl G, Basler K. (1996) Direct and long-range action of a DPP morphogen gradient. Cell 85, 357-368.

Perutz MF, Staden R, Moens L, De Baere I. (1993) Polar zippers. Current Biology 3, 249-253.

Politis EG, Roth AF, Davis NG. (2005) Transmembrane topology of the protein palmitoyl transferase Akr1. Journal of Biological Chemistry. 280, 10156-10163.

Porter JA, Ekker SC, Park WJ, von Kessler DP, Young KE, Chen CH, Ma Y, Woods AS, Cotter RJ, Koonin EV, Beachy PA. (1996) Hedgehog patterning activity: role of a lipophilic modification mediated by the carboxy-terminal autoprocessing domain. Cell 86, 21-34.

Raftery LA, Sutherland DJ. (1999) TGF-β family signal transduction in Drosophila development: from Mad to Smads. Developmental Biology 210, 251-268.

Rocks O, Peyker A, Kahms M, Verveer PJ, Koerner C, Lumbierres M, Kuhlmann J, Waldmann H, Wittinghofer A, Bastiaens PI. (2005) An acylation cycle regulates localization and activity of palmitoylated Ras isoforms. Science 307, 1746-1752.

Rorth P. (1996) A modular misexpression screen in Drosophila detecting tissue-specific phenotypes. Proceedings of the National Academy of Sciences 93, 12418-12422.

Roth AF, Feng Y, Chen L, Davis NG. (2002) The yeast DHHC cysteine-rich domain protein Akr1p is a palmitoyl transferase. Journal of Cell Biology 159, 23-28.

Sanicola M, Sekelsky J, Elson S, Gelbart WM. (1995) Drawing a stripe in Drosophila imaginal disks: negative regulation of decapentaplegic and patched expression by engrailed. Genetics 139, 745-756.

Singaraja RR, Hadano S, Metzler M, Givan S, Wellington CL, Warby S, Yanai A, Gutekunst CA, Leavitt BR, Yi H, Fichter K, Gan L, McCutcheon K, Chopra V, Michel J, Hersch SM, Ikeda JE, Hayden MR. (2002) HIP14, a novel ankyrin domain-containing protein, links huntingtin to intracellular trafficking and endocytosis. Human Molecular Genetics. 11, 2815-2828.

Staehling-Hampton K, Jackson PD, Clark MJ, Brand AH, Hoffmann FM. (1994) Specificity of bone morphogenetic protein-related factors: cell fate and gene expression changes in Drosophila embryos induced by decapentaplegic but not 60A. Cell Growth and Differentiation 5, 585-593.

Sun X, Artavanis-Tsakonas S. (1997) Secreted forms of DELTA and SERRATE define antagonists of Notch signaling in Drosophila. Development 124, 3439-3448.

Tamkun JW, Deuring R, Scott MP, Kissinger M, Pattatucci AM, Kaufman TC, Kennison JA. (1992) brahma: a regulator of Drosophila homeotic genes structurally related to the yeast transcriptional activator SNF2/SWI2. Cell 68, 561-572.

Tamkun JW, Kahn RA, Kissinger M, Brizuela BJ, Rulka C, Scott MP, Kennison JA. (1991) The arflike gene encodes an essential GTP-binding protein in Drosophila. Proceedings of the National Academy of Sciences 88, 3120-3124.

Thummel CS. (1995) From embryogenesis to metamorphosis: the regulation and function of Drosophila nuclear receptor superfamily members. Cell 83, 871-877.

Tsukazaki T, Chiang TA, Davison AF, Attisano L, Wrana JL. (1998) SARA, a FYVE domain protein that recruits Smad2 to the TGFβ receptor. Cell 95, 779-791.

Wu G, Chen YG, Ozdamar B, Gyuricza CA, Chong PA, Wrana JL, Massague J, Shi Y. (2000) Structural basis of Smad2 recognition by the Smad anchor for receptor activation. Science 287, 92-97.

Yanai A, Kang R, Huang K, Singaraja RR, Arstikaitis P, Haigh B, Mullard A, el-Husseini Ael-D, Hayden MR. (2005) Decreased palmitoylation of mutant huntingtin leads to disturbed trafficking and increase toxicity. Submitted.

Zhai L, Chaturvedi D, Cumberledge S. (2004) Drosophila wnt-1 undergoes a hydrophobic modification and is targeted to lipid rafts, a process that requires porcupine. Journal of Biological Chemistry 279, 33220-33227.

Yu K, Srinivasan S, Shimmi O, Biehs B, Rashka KE, Kimelman D, O'Connor MB, Bier E. (2000) Processing of the Drosophila Sog protein creates a novel BMP inhibitory activity. Development 127, 2143-2154.

Zheng X, Wang J, Haerry TE, Wu AY, Martin J, O'Connor MB, Lee CH, Lee T. (2003) TGF-β signaling activates steroid hormone receptor expression during neuronal remodeling in the Drosophila brain. Cell 112, 303-315.